Phys. **43**, 3080 (1965)] concludes that the temperature dependence of the three-body conversion to form He_2^+ may range between $T^{-5/4}$ at low temperatures to $T^{-1/4}$ at high temperature. G. R. Hays and H. J. Oskam (private communication) have found that the temperature dependence of the reaction-rate constant is small in the range 120–300 °K.

[15]The three-body rate coefficient β for the process $Cs^+ + 2Cs \rightarrow Cs_2^+ + Cs$ was estimated by the authors (Ref. 2) to be $\beta \simeq 6 \times 10^{-29}$ cm^6/sec. A calculation of the coefficient using the equation derived by Bruce H. Mahan [J. Chem. Phys. **43**, 3080 (1965)] yields a value of $\beta \simeq 10^{-29}$ cm^6/sec. This calculation of β depends upon the charge exchange cross section. A value of the cross section, $Q_{CE} \simeq 7 \times 10^{-14}$ cm^2, was extrapolated from the data of W. R. Gentry, Yuan-Tseh Lee, and Bruce H. Mahan [J. Chem. Phys. **49**, 1758 (1968)]. The only other reported value of the coefficient, $\beta \simeq 10^{-26}$ cm^6/sec, was given by N. D. Morgulis and Yu. P. Korchevoi {Zh. Eksp. Teor. Fiz. Pis'ma Red. **9**, 313 (1968) [JETP Lett. **8**, 192 (1968)]}.

[16]J. R. Peterson and D. C. Lorents, Phys. Rev. **182**, 152 (1969).

[17]A. S. Schlachter, D. H. Lloyd, P. J. Bjorkholm, and L. W. Anderson, Phys. Rev. **174**, 201 (1968).

[18]B. L. Donnally and G. Thoeming, Phys. Rev. **159**, 87 (1967).

[19]D. K. Bohme, N. G. Adams, M. Mosesman, D. B. Dunkin, and E. E. Ferguson, J. Chem. Phys. **52**, 5094 (1970).

[20]G. Gioumousis and D. P. Stevenson, J. Chem. Phys. **29**, 294 (1958).

[21]G. E. Chamberlain and J. C. Zorn, Phys. Rev. **129**, 677 (1963).

[22]W. P. Sholette and E. E. Muschlitz, Jr., J. Chem. Phys. **36**, 3368 (1962).

[23]K. L. Bell, A. Dalgarno, and A. E. Kingston, J. Chem. Phys. **36**, 3368 (1962).

[24]P. Langevin, Ann. Chim. Phys. **5**, 245 (1905).

[25]The value of the dielectric coefficient of helium was taken from the *American Institute of Physics Handbook*, 2nd ed. (McGraw-Hill, New York 1963).

[26]A. M. Tyndall, *The Mobility of Positive Ions in Gases* (Cambridge U. P., Cambridge, England, 1938).

[27]A. P. Vitols and H. J. Oskam (private communication).

[28]R. Johnson and M. A. Biondi, Gaseous Electronics Conference, London, Ontario, 1972 (unpublished).

PHYSICAL REVIEW A VOLUME 8, NUMBER 2 AUGUST 1973

Carrier-Frequency Distance Dependence of a Pulse Propagating in a Two-Level System*

J. C. Diels† and E. L. Hahn

Department of Physics, University of California, Berkeley, California 94720

(Received 11 January 1973)

A study is made of the distance dependence of carrier phase and average frequency of an electromagnetic pulse propagating through a quantum two-level system. Phenomenological differential equations are introduced to describe the distance rate of change of first- and second-moment deviations of the pulse carrier frequency from its original input frequency. In equilibrium the equations predict characteristics of pulse propagation in steady state. For both absorber and amplifier cases, computer plots are presented of the distance dependence of pulse shape, carrier phase, Fourier amplitude, and pulse energy for selected types of homogeneous and inhomogeneous line broadening and for specific input-pulse conditions. Off-resonance formation of a single 2π hyperbolic secant pulse of self-induced transparency may evolve from input-pulse areas less than π, as well as slightly greater than π, accompanied by frequency modulation and pulse breakup. The amplification of pulsed carrier radiation is accompanied by frequency pulling toward resonance. With and without phase modulation, stability conditions for stable pulse propagation are obtained. Either frequency pulling toward or frequency pushing away from resonance is dominant for an absorber, according to the dominance, respectively, of homogeneous or inhomogeneous line broadening. In the slowly-varying-pulse-envelope approximation, a steady-state solution is found for a symmetrically-phase-modulated pulse propagating in an amplifier with scattering losses. The mean carrier frequency for the pulse is displaced off resonance by one linewidth above the resonance transition frequency of a homogeneously broadened system.

I. INTRODUCTION

Little attention has been given to the distance dependence of carrier frequency and phase changes of traveling-wave radiation as it interacts nonlinearly with a medium which contains dipole transitions on or off resonance with respect to the carrier frequency. Cumulative carrier-frequency shifts and spectral changes can result over long distances of propagation. In the far-off-resonance case, significant effects are expected if an infinitely extended medium acts as an amplifier, with excited quantum states populated in excess over lower states by virtue of some external pumping mechanism. The initial off-resonance carrier frequency is expected to pull toward the transition frequency of the inverted system as the distance of propagation increases. In the case of an absorbing medium the spectral changes in the radiation are of quite a different nature, particularly when the radiation is in the form of a pulse. These changes occur if the applied carrier frequency is

very near the resonance transition frequency of the absorber. They may be observed before the radiation has been completely absorbed because of incoherent scattering and damping mechanisms. In the case of an emissive medium, if the input-radiation power gain exceeds scattering losses, the radiation will propagate over very long distances as the power gain and losses come into balance.

In this paper we introduce phenomenological and computer calculations to show under limited conditions that nonlinear spectral changes can occur. Cases are presented[1] which describe the distance dependence of spectral changes correlated with initial conditions. The model applied is a two-quantum-level system interacting with a single or nearly single frequency radiation source in the form of a pulse. In certain circumstances the pulse may be descriptive of continuous wave radiation in the limit of infinite pulse width. Although this simplified two-quantum-level model is not sufficiently realistic to apply generally to predictions concerning possible modifications of interstellar spectra, it raises the question whether or not in some isolated cases interstellar radiation spectra might be affected by nonlinear interactions with matter over long propagation distances. Our results have more direct applicability to the pulse behavior in laser amplifiers where the pulse carrier frequency is initially applied near the transition frequency of the active laser medium.

The semiclassical treatment of pulse propagation in the analysis of self-induced transparency[2] (SIT) showed that phase modulation could be assumed absent if a single carrier frequency within a pulse envelope is applied at the exact resonance transition frequency of a quantum two-level system. The spectrum of the system is chosen to be symmetrically and inhomogeneously broadened, and is incorporated into the Bloch–Maxwell equations, using the slowly-varying-wave approximation. After entering the medium the pulse changes in shape, intensity, and delay as a function of propagation distance, but remains free of phase modulation because of the chosen initial conditions. For distances large compared to the classical absorption length, the pulse maintains a distortionless equilibrium 2π hyperbolic secant (h. s.) shape. The pulse area 2π, proportional to the product of field amplitude and pulse duration, here signifies that the first π portion of induced absorption is balanced by the second π portion of induced emission, leaving both the pulse and medium with no net change in energy. This ideal description applies only in the absence of incoherent damping effects, involving nondegenerate or special types of two-level states, and for complete forward scattering of an infinite plane wave and minimal or zero backscattering.

In real physical situations, a number of the above idealizations are violated to some extent. Here we are particularly interested in two-level systems more likely to be excited off resonance than on resonance by pulses which may be initially phase modulated as well. As a result of these initial conditions, the phase and carrier frequency of propagating pulses will also become a function of time and distance, because of nonlinear energy exchange between radiation and medium.

II. DISTANCE DEPENDENCE OF AVERAGE CARRIER FREQUENCY

It will be convenient to develop a description of the distance dependence of the average pulse carrier frequency while retaining some of the assumptions[2] used to describe SIT. With the initial carrier frequency ω of the pulse now not necessarily at the exact resonance of a symmetric inhomogeneously broadened line, the propagating wave is defined as

$$E(z,t) = \mathcal{E}(z,t)\, e^{i[\omega t - kz + \varphi(z,t)]} + \text{c. c.} \quad , \tag{1}$$

where the instantaneous carrier frequency is $\omega(t) = \omega + \dot{\varphi}(z,t)$. Averaging $\dot{\varphi}(z,t)$ over the pulse, the average carrier frequency is given by

$$\omega_{av} = \omega + \langle \dot{\varphi}(z) \rangle \quad , \tag{2}$$

with

$$\langle \dot{\varphi}(z) \rangle = \frac{\int_{-\infty}^{\infty} \dot{\varphi}(z,t)\mathcal{E}^2(z,t)\,dt}{\int_{-\infty}^{\infty} \mathcal{E}^2(z,t)\,dt} = \frac{\int_{-\infty}^{\infty} \Omega\, |\tilde{\mathcal{E}}(z,\Omega)|^2\, d\Omega}{\int |\tilde{\mathcal{E}}(z,\Omega)|^2\, d\Omega} = \langle \Omega \rangle \tag{3}$$

and

$$\tilde{\mathcal{E}}(z,\Omega) = \int_{-\infty}^{\infty} \mathcal{E}(z,t)\, e^{i\Omega t + i\varphi(z,t)}\, dt \quad . \tag{4}$$

The average frequency shift $\langle \dot{\varphi}(z) \rangle = \langle \Omega \rangle$ is therefore the first moment of the pulse Fourier spectrum, which follows for a finite pulse envelope $\mathcal{E}(z,t)$.

In terms of

$$\langle \dot{\varphi}^2(z) \rangle = \frac{\int_{-\infty}^{\infty} \dot{\varphi}^2(z,t)\mathcal{E}^2(z,t)\,dt}{\int_{-\infty}^{\infty} \mathcal{E}^2(z,t)\,dt} \quad , \tag{5}$$

the second moment is defined as

$$\langle \Omega^2 \rangle = \frac{\int_{-\infty}^{\infty} \Omega^2\, |\tilde{\mathcal{E}}(z,\Omega)|^2\, d\Omega}{\int_{-\infty}^{\infty} |\tilde{\mathcal{E}}(z,\Omega)|^2\, d\Omega} = \langle \dot{\varphi}^2(z) \rangle + \frac{\int_{-\infty}^{\infty} \dot{\mathcal{E}}^2(z,t)\,dt}{\int_{-\infty}^{\infty} \mathcal{E}^2(z,t)\,dt} \quad . \tag{6}$$

For a bell-shaped pulse envelope,

$$\frac{\int_{-\infty}^{\infty} \dot{\mathcal{E}}^2(z,t)\,dt}{\int_{-\infty}^{\infty} \mathcal{E}^2(z,t)\,dt} = \frac{1}{\tau^2} \tag{7}$$

is a measure of the reciprocal mean square of the

pulse width (in $\sec^{-2}$).

The above definitions will be connected with the semiclassical Bloch–Maxwell equations:

$$\frac{\partial u}{\partial t} = (\Delta\omega - \dot{\varphi})v - \frac{u}{T_2} \quad , \tag{8}$$

$$\frac{\partial v}{\partial t} = -(\Delta\omega - \dot{\varphi})u - \frac{\kappa^2}{\omega_0}\mathcal{E}W - \frac{v}{T_2} \quad , \tag{9}$$

$$\frac{\partial W}{\partial t} = \omega_0 \mathcal{E} v \quad , \tag{10}$$

$$\frac{\partial \mathcal{E}}{\partial z} + \frac{\eta}{c}\frac{\partial \mathcal{E}}{\partial t} = \frac{-2\pi\omega}{\eta c}\int_{-\infty}^{\infty} v g(\delta)\, d\delta \quad , \tag{11}$$

$$\mathcal{E}\frac{\partial \varphi}{\partial z} + \frac{\eta}{c}\mathcal{E}\frac{\partial \varphi}{\partial t} = \frac{-2\pi\omega}{\eta c}\int_{-\infty}^{\infty} u g(\delta)\, d\delta \quad . \tag{12}$$

The polarization components u and v are understood to be functions of z, t, and the particular off-resonance frequency difference $\Delta\omega$. These components are, respectively, in phase and 90° out of phase with the direction of the slowly varying modulus field $\mathcal{E}(z,t)$ which rotates at the instantaneous frequency $\omega + \dot{\varphi}(z,t)$, where $E(z,t)$ is chosen[2] to represent a circularly polarized wave. Only the phenomenological damping term $1/T_2$ is included above. The energy expectation value of the number density N of the two-level system is given by W. The vacuum wavelength is $\lambda_0 = 2\pi c/\omega$, and the background refractive index η of the medium is assumed unaffected by the pulse. The dipole moment of the transition is p_0, defined in $\kappa = 2p_0/\hbar$, and $g(\delta)$ is the inhomogeneous spectral distribution function.

Figure (1) is a spectrum schematic showing the parameters associated with off-resonance pulse propagation. For an initial pulse at $z=0$, not phase modulated, the off-resonance parameter is $\Delta\omega = \omega_0 + \delta - \omega = \Delta\omega_0 + \delta$. The inhomogeneous spectrum distribution function is chosen, for example, to be

$$g(\delta) = (T_2^*/\sqrt{\pi})\, e^{-\delta^2 T_2^{*2}} \quad . \tag{13}$$

A. First-Moment Equation

An expression for $d\langle\dot{\varphi}\rangle/dz$ is sought by taking the first derivative of Eq. (3) and combining it with Eqs. (8)–(12). The following conditions are applied, with the pulse maximum defined at $t=0$ for $z=0$:

$$\begin{aligned} &\mathcal{E}(z,t) = 0 && \text{at } t = \pm\infty \quad , \\ &u = v = 0 && \text{at } t = -\infty \quad , \\ &W_0(\delta) = \pm\tfrac{1}{2}N\hbar\omega_0 g(\delta) && \text{at } t = -\infty \quad , \\ &\Delta W(\delta) = W(z,\delta) - W_0(\delta) && \text{at } t = +\infty \quad . \end{aligned} \tag{14}$$

The minus sign is chosen for an absorber and the plus sign for an emitter in the definition of $W_0(\delta)$. The inhomogeneous spectral width $\sim 1/T_2^*$ [e.g., Eq. (13)] is sufficiently small so that the ground-state energy $\sum_\delta W(\delta) = -\frac{1}{2}(N\hbar\omega_0)$ at $t=-\infty$ may be specified in terms of the mean transition frequency ω_0. The energy absorbed or emitted by the two-level system at position z is expressed as $\Delta W(\delta)$ after the pulse subsides at $t=+\infty$, where

$$\Delta W(\delta) = \omega_0 \int_{-\infty}^{\infty} v(\delta, z, t)\mathcal{E}(z,t)\, dt \tag{15}$$

is understood to be a function of z. The result for $d\langle\dot{\varphi}\rangle/dz$ is

$$\frac{d\langle\dot{\varphi}\rangle}{dz} = \frac{-1}{\mathcal{T}(z)}\frac{\omega}{\omega_0}\int_{-\infty}^{\infty}\Delta W(\delta)(\Delta\omega - \langle\dot{\varphi}\rangle)g(\delta)d\delta + \frac{2\langle k'\rangle}{T_2} \quad , \tag{16}$$

where $\langle\dot{\varphi}\rangle$ and $\langle k'\rangle$ are also functions of z. The pulse energy is

$$\mathcal{T}(z) = \frac{\eta c}{4\pi}\int_{-\infty}^{\infty}\mathcal{E}^2(z,t)\, dt \quad . \tag{17}$$

The average contribution to the propagation vector because of the two-level system is given by

$$\begin{aligned}\langle k'\rangle &= -\left(\int_{-\infty}^{\infty}\mathcal{E}^2\frac{\partial\varphi}{\partial z}\,dt\right)\Big/\int_{-\infty}^{\infty}\mathcal{E}^2\,dt \\ &= \frac{\omega}{2\mathcal{T}}\int_{-\infty}^{\infty}\int_{-\infty}^{\infty} u\mathcal{E}\, g(\delta)\, d\delta\, dt \quad . \end{aligned} \tag{18}$$

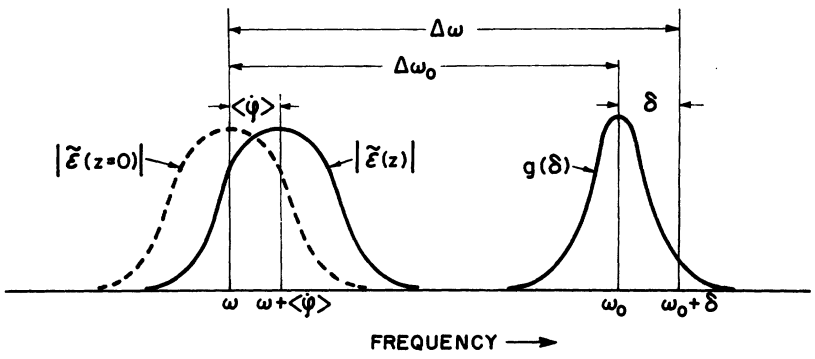

FIG. 1. Schematic of spectral amplitudes of the pulse at initial ($z=0$) frequency ω, at final ($z=\infty$) average frequency $\omega+\langle\dot{\varphi}\rangle$, and resonance line at frequency ω_0, showing parameters and sign conventions. A pulse off resonance signifies that $\Delta\omega_0 \neq 0$.

Appendix A presents Eqs. (10)–(12) in greater generality for later reference, together with a short discussion on the origin of neglected higher-order terms. The slowly-varying-envelope approximation is justified under the conditions $\partial\mathcal{E}/\partial t \ll \omega\mathcal{E}$ and $\partial\mathcal{E}/\partial z \ll k\mathcal{E}$. The resulting equations (11) and (12) for the forward-traveling wave are valid only if $\Delta\omega/\omega \ll 1$ and $\dot{\varphi}/\omega \ll 1$. These restrictions may be removed and replaced by next-higher-order restrictions $(\Delta\omega/\omega)^2 \ll 1$, $\dot{\varphi}/2\omega \ll 1$, together with $\kappa\mathcal{E}/\omega$, $1/\omega T_2^*$, $\ddot{\varphi}/\omega^2$, $\ddot{u}/\omega^2 u$, $1/\omega T_2$, and $\ddot{v}/\omega^2 v \ll 1$ by simply making the following replacements:

$$z \to \left(\frac{\omega + 2\Delta\omega_0}{\omega}\right) z \ , \qquad t \to t + \left(\frac{2\Delta\omega_0}{\omega}\right)\frac{\eta z}{c} \ ,$$

and

$$\sigma \to \frac{\omega}{\omega + 2\Delta\omega_0}\,\sigma \ .$$

These replacements are valid for $1/\omega T_2^* \ll 1$. These changes apply to laboratory frames z and t. The t transformation need not be applied to plots given later where the retarded-time axis of reference $t - \eta z/c$ is used. However, the transformation for z is still necessary. A scattering parameter σ is introduced later in a damping term $-\sigma\frac{1}{2}(\mathcal{E})$ to be added to the right-hand side of Eq. (11). This parameter does not affect Eq. (16).

B. Second-Moment Equation

An expression for an equation involving $d\langle\dot{\varphi}^2\rangle/dz$ is derived in Appendix B. The procedure is tedious but similar to that for obtaining Eq. (16), except that one works with the z derivative of Eq. (5) instead of Eq. (3). The scattering-loss term $-\sigma\frac{1}{2}(\mathcal{E})$ is added to the right-hand side of Eq. (11), and therefore a term involving σ appears below, to be referred to later. Therefore we have

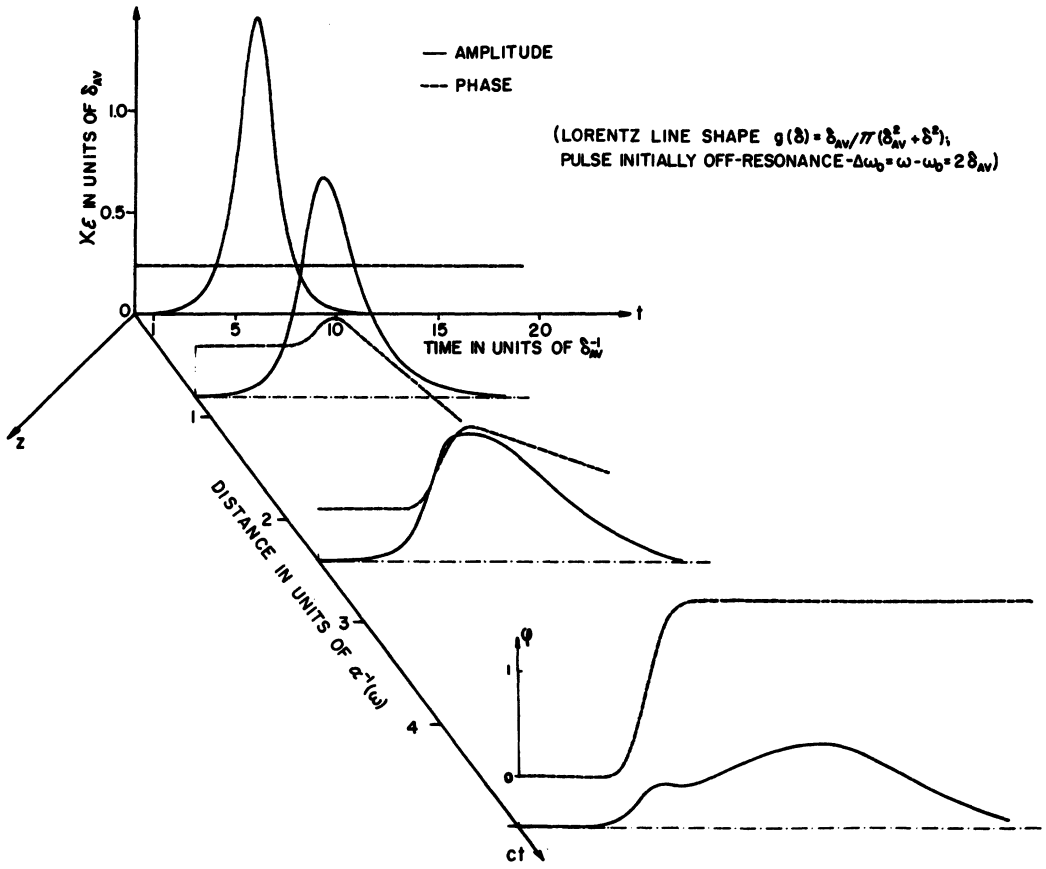

FIG. 2. Propagation of a pulse (initially two linewidths above resonance) through a Lorentz-broadened medium. The initial pulse area is $\Theta_0 = 3.64$. The pulse is initially unchirped and h. s. shaped [pulse shape: sech$(t/0.8)$]. In all figure captions to follow, t is in units of δ_{AV}^{-1}. The linear phase shift due to constant wave vector has been subtracted.

$$\frac{d\langle\dot{\varphi}^2\rangle}{dz}=\frac{1}{\mathcal{T}}\left\{\int_{-\infty}^{\infty}\int_{-\infty}^{\infty}dt\,d\delta\,g(\delta)\left[\omega v\mathcal{E}\left(\langle\dot{\varphi}^2\rangle+\frac{1}{T_2^2}-\Delta\omega^2\right)+\frac{\omega}{\omega_0}\kappa^2\mathcal{E}^2\left(\frac{W}{T_2}-\frac{\dot{W}}{2}\right)+\frac{2\omega\delta\mathcal{E}u}{T_2}\right]\right\}$$
$$+4\frac{\Delta\omega_0}{T_2}\langle k'\rangle-\frac{1}{\mathcal{T}}\left[\frac{d}{dz}\left(\frac{\mathcal{T}}{\tau^2}\right)+\frac{\sigma\mathcal{T}}{\tau^2}\right]\ . \tag{19}$$

III. CASE OF AN ABSORBER

A. Evolution toward Self-Induced Transparency

The ideal limit of SIT can be deduced from Eq. (16) for no damping and no scattering ($T_2=\infty$, $\sigma=0$). Equations (10) and (11), together with (17), lead to the conservation equation

$$\frac{d\mathcal{T}}{dz}=-\int_{-\infty}^{\infty}\Delta W(\delta)\,g(\delta)\,d\delta\ , \tag{20}$$

letting $\omega_0\approx\omega$. Coupling Eq. (20) to (16) gives the result

$$\mathcal{T}(z)[\Delta\omega_0-\langle\dot{\varphi}(z)\rangle]-\mathcal{T}(0)[\Delta\omega_0-\langle\dot{\varphi}(0)\rangle]$$
$$=\int_0^z\int_{-\infty}^{\infty}\delta\Delta W(\delta)g(\delta)\,d\delta\,dz\ . \tag{21}$$

If $\langle\dot{\varphi}(0)\rangle=0$ and a 2π h. s. -shaped pulse enters the medium at $z=0$, then from SIT, $\Delta W(\delta)=0$, $\mathcal{T}(z)=\mathcal{T}(0)$, and therefore $\langle\dot{\varphi}(z)\rangle=0$ for all z. Also, for T_2 finite, Eq. (16) shows for a pulse applied at exact resonance ($\Delta\omega_0=0$) that it is consistent to fix $\langle\dot{\varphi}(z)\rangle=0$ for all z if $\langle\dot{\varphi}(0)\rangle=\dot{\varphi}(z,t)=0$. This will follow from Eq. (16) if $g(\delta)$ is an even function of δ, and therefore permits v and W to be even in δ, and u to be defined odd in δ, referring to Eqs. (8)–(12). If $\ddot{\varphi}(z,t)\neq0$, these properties of even and odd in δ cannot be assigned to u, v, and W. Although computer solutions will show later that a propagating 2π h. s. pulse is stable against phase modulation for an inhomogeneously broadened system, this stability property has not been proved analytically. The self-consistency argument above is of no help in this regard.

If $\langle\dot{\varphi}(0)\rangle=0$ and $\Delta\omega\neq0$ [$g(\delta)$ not symmetric in δ also has the same effect], or if $\langle\dot{\varphi}(0)\rangle\neq0$ and $\Delta\omega=0$ (or $\neq0$), inspection of Eqs. (16) and (21) shows that a finite value of $\langle\dot{\varphi}(z)\rangle$ will develop. The parameters sketched in Fig. 1 relate to Eq. (16) by taking $\Delta\omega=\omega_0-\omega$ positive for a pulse carrier frequency applied initially below resonance. Equation (16) implies that $d\langle\dot{\varphi}\rangle/dz$ is initially negative if $\Delta\omega>\langle\dot{\varphi}\rangle$, $\ddot{\varphi}=0$, and $T_2=\infty$. From Eq. (2) the average carrier frequency ω_{av} therefore recedes from the resonance line at ω_0. Similarly, this happens for negative $\Delta\omega_0$, when the pulse is applied above resonance.

In the limit $d\langle\dot{\varphi}\rangle/dz\to0$ for z large, Eqs. (16) and (21) imply that a pulse of initial arbitrary shape may loose a finite amount of energy $\mathcal{T}(z)-\mathcal{T}(0)$. We let $T_2=\infty$. This net energy loss is divided up into energy which must account for a change in average carrier frequency and energy which is required to excite the two-level system. The final value of $\mathcal{T}(z)$ might be expected to be zero as $z\to\infty$. Indeed, according to Eqs. (16) and (21), a phase modulation (chirp) develops for nonresonant imput pulses, and only stationary 2π h. s. pulses are free of phase modulation. One would therefore be tempted to conclude the self-induced transparency cannot develop because it would be unstable against frequency detuning unless only 2π h. s. pulses are initially applied to the sample. A computer analysis shows that this conclusion is incorrect. Bell-shaped-type input pulses of arbitrary shape and area can produce unmodulated 2π h. s. pulses, even off resonance, as seen in Figs. 2–5. The pulse spectra corresponding to Figs. 2 and 3 are, respectively, displayed as a function of three propagation-distance points in Figs. 4 and 5. Figures 2 and 3 show that a smaller part of the initial pulse breaks away at its own velocity $\lesssim c/\eta$, leaving the remaining pulse portion behind, which evolves toward a 2π h. s. pulse of width τ, with a slower pulse velocity[2] $V\sim\frac{1}{2}\alpha\tau^{-1}$, where α is the classical absorption coefficient. The delayed second pulse envelope of Fig. 3 fits a 2π h. s. width of $2.5\delta_{AV}^{-1}$ sec, where δ_{AV} is the inhomogeneous linewidth. The smaller pulse with velocity $\lesssim c/\eta$ possesses a phase modulation which causes its mean frequency to move away from ω_0 with increasing z, while at the same time its intensity decreases toward zero. The remainder of the pulse, which ultimately becomes a 2π h. s. shape, first shows a tendency[3] to pull toward the resonance at ω_0, but finally returns to the original input frequency ω as the 2π h. s. condition is reached at large z. The first moment $\langle\dot{\varphi}\rangle$ of these two pulses in combination still obeys the requirement that $\langle\dot{\varphi}\rangle$ initially recedes from ω_0 with increasing z for an absorber, according to Eq. (16) ($T_2=\infty$). The final pulse energy of the 2π h. s. pulse which remains is

$$\mathcal{T}(\infty)=\mathcal{T}(0)\,e^{-R(z=\infty)}\ , \tag{22}$$

where

$$R=\int_0^{z=\infty}\int_{-\infty}^{\infty}\frac{\delta\Delta W(\delta)\,g(\delta)\,d\delta\,dz}{\mathcal{T}(z)[\Delta\omega_0-\langle\dot{\varphi}(z)\rangle]}\ . \tag{23}$$

The expressions "frequency pulling" and "frequency pushing" will be used to indicate, respectively, the change of carrier frequency toward and away from the resonance line at ω_0. The computer plots of Figs. 2 and 3 show distinctive trends in frequency modulation at the leading and lagging edges of the pulse near $z=0$. The leading edge shows that $\omega+\dot{\varphi}$ pulls away from ω_0, while the $\omega+\dot{\varphi}$ of the lagging edge pushes toward ω_0. In fact, for $t\to+\infty$, the tail of the pulse oscillates at the frequency ω_0 itself. This latter behavior is justifiable, because the two-level system is left excited and radiates at its own transition frequency after the driving pulse subsides. The leading edge of the pulse shows an opposite behavior because of a transient nonlinear dispersive effect. For the slowly rising portion of $\mathcal{E}(z,t)$, where the absorbers respond adiabatically to the field during the condition $\Delta\omega \gg \kappa\mathcal{E}$, then u is proportional to $\mathcal{E}$, $\partial\varphi/\partial z$ is a constant in Eq. (12), and $\dot{\varphi}=0$. The $\dot{\varphi}$ term of Eq. (12) may be omitted in the retarded-time frame of reference, where t is replaced by $t-\eta z/c$. As $\mathcal{E}(z,t)$ rises rapidly, u can no longer follow in proportion to $\mathcal{E}$, which means from the equivalent "precession" picture that the effective polarization vector, of magnitude $\kappa W_0/\omega_0$, tends to precess around an effective field $[\mathcal{E}^2+(\Delta\omega/\kappa)^2]^{1/2}$. The effective polarization vector produces a projection polarization component u which now increases faster than $\mathcal{E}$. Depending upon the sign of $\Delta\omega_0$, the time rate of change of $\partial\varphi/\partial z$ is such that frequency pushing occurs in the beginning of the pulse. On the other hand, if T_2 is very short, and $2\langle k'\rangle/T_2$ is the dominant term in Eq. (16), the opposite effect occurs, and the carrier frequency pulls toward ω_0 for an absorber. This follows from classical arguments, where line saturation below resonance ($\omega<\omega_0$), for example, causes a decrease in the refractive index and a corresponding increase in the wave velocity. With $2\langle k'\rangle/T_2$ dominant for an emitter the opposite behavior is predicted for short propagation distances. Ultimately the carrier frequency is pulled toward ω_0 for the emitter case (to be shown later).

In the case of a Lorentzian absorption line (Fig. 2), with far-out wings in its spectrum, the "fast pulse" moving at velocity $\lesssim c/\eta$, resulting from the early phase modulation, has its Fourier components subjected to absorption in the spectral wings, and will be absorbed quickly after a finite propagation distance. In the case of a shorter pulse applied to a Gaussian line (Fig. 3) with spectral wings not as far out, the pulse modulation occurs in a much shorter distance than in the Lorentz

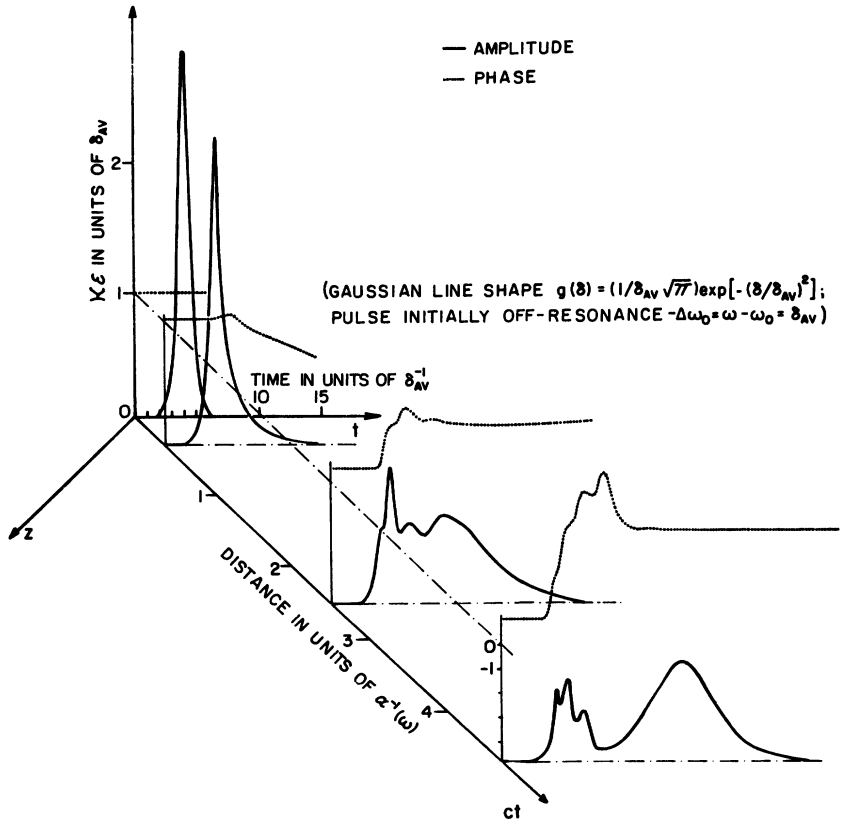

FIG. 3. Propagation of a short pulse (initially one linewidth above resonance) through a Gaussian-broadened medium. The initial pulse area is $\Theta_0=3.64$. The pulse is initially unchirped and h.s. shaped [pulse shape: sech(t/0.4)].

case, because the Gaussian line shape falls off faster as a function of frequency. In this case the "fast pulse" is hardly attenuated over a long distance because it has Fourier components mostly outside of the Gaussian line spectrum.

The general behavior of a "fast pulse" separating from the mean pulse remains qualitatively the same when the pulse is applied initially far off resonance. In the case shown in Fig. 6, the initial frequency of the pulse is four linewidths away from the absorbing line. Since the Fourier components of the pulse and the absorbing line overlap much less in this case, the propagation distance required to form the 2π h. s. pulse is much greater. Figures 7 and 8 show plots of pulse energy, average carrier frequency, and Fourier amplitude versus distance z for the two cases plotted in Figs. 2 and 3, respectively. Again, for reasons of greater overlap between pulse and line spectrum in the Lorentz case than in the Gaussian case, there is a faster return of ω_{av} toward ω in Fig. 7 than in Fig. 8, although the approach toward a 2π h. s. pulse is conversely slower. No clear dynamical argument can be given to explain the latter. Energetically one might argue that more pulse energy remains available in the Gaussian case to be converted more rapidly into a 2π h. s. -shaped pulse.

From our computer data (not shown in any of the figures) we find that the stabilization of the 2π h. s. pulse at the original frequency ω occurs over a narrow time region during the pulse, where the average value of $\dot{W}$ switches sign. The average of u is then near its maximum value and is momentarily proportional to the field $\mathcal{E}(z,t)$, when $\dot{W}$ passes through zero. It is around this time point that the symmetry of a future 2π h. s. develops, when the transition from induced absorption to induced emission takes place.

B. Small- and Large-Signal Behavior of $d\langle\dot{\varphi}\rangle/dz$

Expressions can be obtained for the initial rate, $d\langle\dot{\varphi}\rangle/dz|_{z_0}$ at $z=z_0$, where $\mathcal{E}(z_0,t)$ and $\dot{\varphi}(z_0)$ are given, and $T_2=\infty$. The approximation

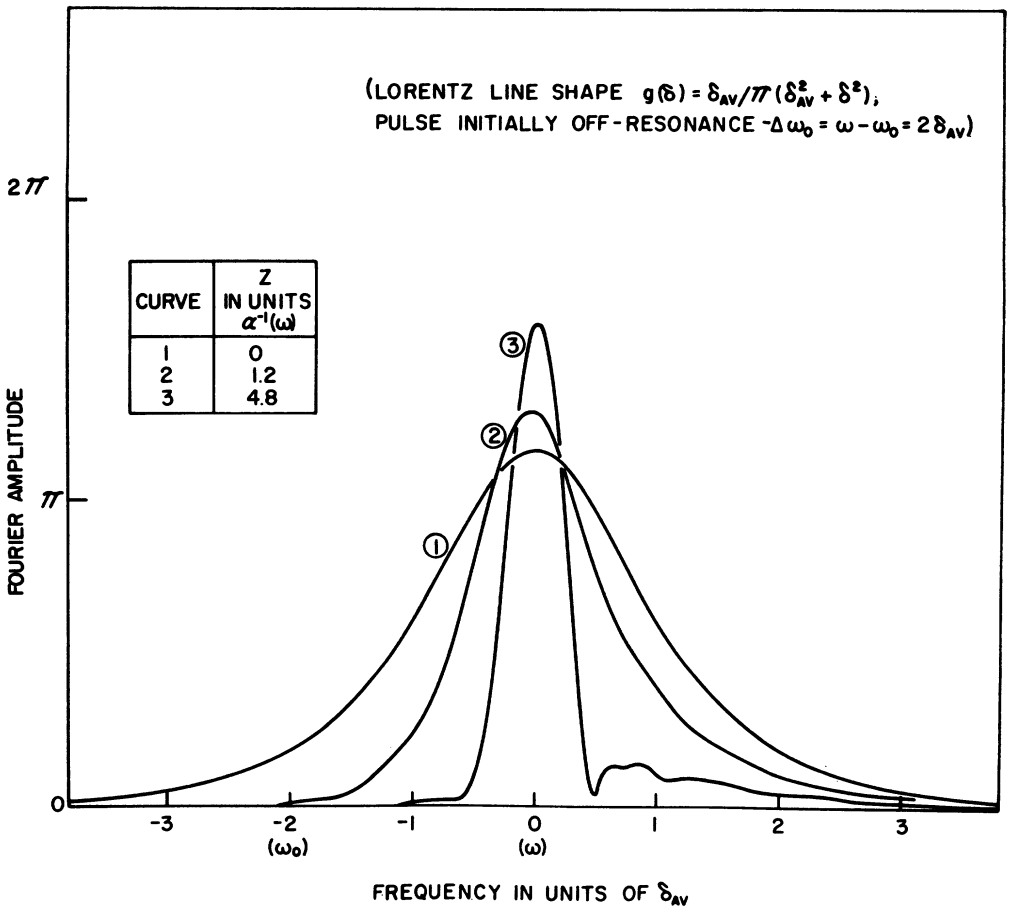

FIG. 4. Fourier amplitude of the pulses shown in Fig. 2 for three propagation-distance points. $\alpha^{-1}(\omega)$ is the absorption coefficient at initial frequency ω.

$$\int_{-\infty}^{\infty} W(\delta, z_0, t=\infty) g(\delta)\, d\delta \simeq W_0$$

can be made if $\mathcal{E}(z_0, t)$ is small. Equations (8) and (9) yield the solution

$$|u(z_0, \Delta\omega, t=\infty) - iv(z_0, \Delta\omega, t=\infty)|^2 = \left(\frac{\kappa^2}{\omega}\right)^2 \left| \int_{\infty}^{\infty} \mathcal{E} W e^{-i[\Delta\omega t' - \varphi(t')]}\, dt' \right|^2 . \quad (24)$$

In the small-signal approximation, it follows that

$$W^2 - W_0^2 \approx 2W_0 \Delta W \ , \quad (25)$$

from the conservation relation

$$\left(\frac{\kappa}{\omega}\right)^2 W^2 + u^2 + v^2 = \left(\frac{\kappa}{\omega}\right)^2 W_0^2 \ . \quad (26)$$

Therefore, combining Eqs. (24), (25), and (26) gives

$$\Delta W = -\tfrac{1}{2}(\kappa^2 W_0) |\tilde{\mathcal{E}}(\Delta\omega)|^2 \ , \quad (27)$$

where $\tilde{\mathcal{E}}(\Delta\omega)$ is the Fourier transform defined in Eq. (4) and $\Delta\omega$ here is redefined as $\Delta\omega = \omega_0 - \omega - \langle\dot{\varphi}(z_0)\rangle + \delta$.

Introducing a δ function for the inhomogeneous broadening, and combining Eq. (27) with Eq. (16), one finds the weak-pulse sharp-line limit for the frequency pushing to be

$$\left.\frac{d\langle\dot{\varphi}\rangle}{dz}\right|_{z_0} = 2\pi\left(\frac{\kappa^2 W_0}{\eta c}\right) \Delta\omega_0 F(\Delta\omega_0) \ , \quad (28)$$

where $F(\Omega) = (\eta c/4\pi)|\tilde{\mathcal{E}}^2(\Omega)|/\mathcal{T}$ is the normalized spectral power density. All terms in (28) are understood to apply at $z = z_0$. The initial frequency pushing can also be evaluated analytically for an inhomogeneously broadened line in the weak-pulse-signal approximation. Suppose we choose a Gaussian pulse spectrum

$$|\tilde{\mathcal{E}}(\Omega)|^2 = \frac{\Theta^2\tau^2}{\kappa^2} e^{-\Omega^2\tau^2} \ , \quad (29)$$

where Θ is the assigned area of the pulse and τ is the pulse width. The inhomogeneous spectrum of $g(\delta)$ given by Eq. (13) is chosen in evaluating the integration over δ in Eq. (16). The result is

$$\left.\frac{d\langle\dot{\varphi}\rangle}{dz}\right|_{z_0} = 4\pi^{3/2}\left(\frac{\kappa^2 W_0}{\eta c}\right) \Delta\omega_0 \tau s^3 e^{-\Delta\omega_0^2\tau^2 s^2} , \quad (30)$$

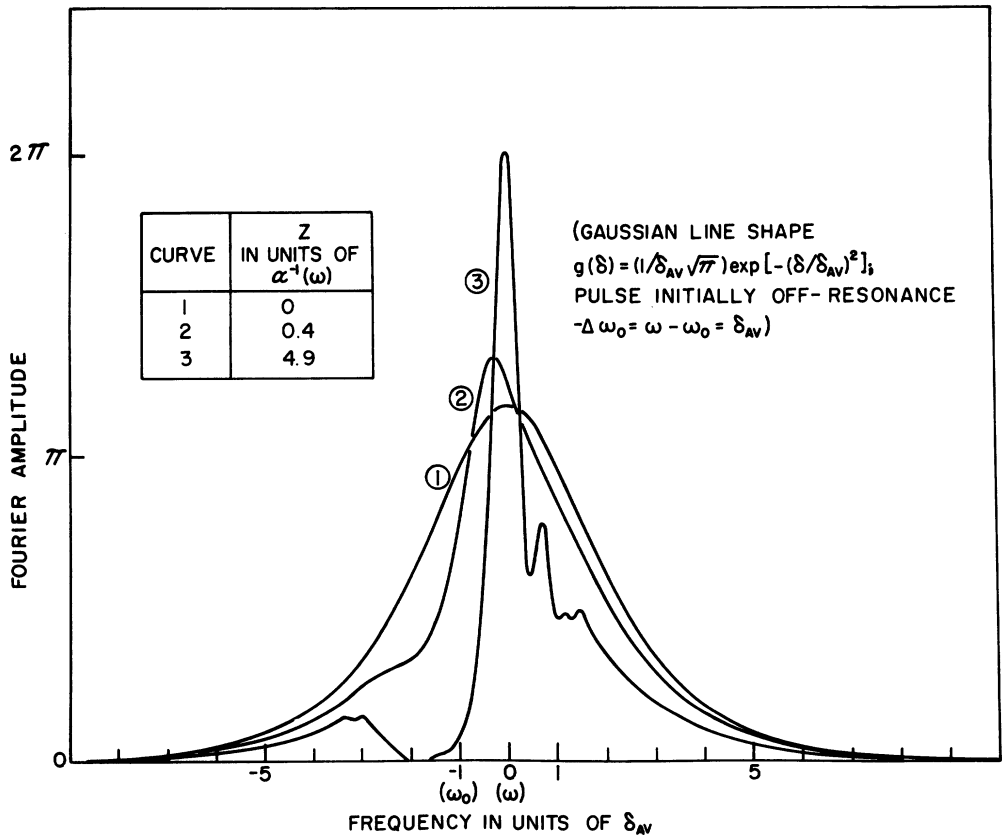

FIG. 5. Fourier amplitude of the pulses shown in Fig. 3 for three propagation-distance points.

where

$$s = \frac{T_2^*}{(T_2^{*2} + \tau^2)^{1/2}} \quad . \tag{31}$$

The maximum of this function (at $\Delta\omega_0\tau = 1/s\sqrt{2}$) is proportional to s^2. The highest "frequency pushing" occurs therefore in the sharp-line limit ($s = 1$).

In the case of weak pulses, $d\langle\dot{\varphi}\rangle/dz|_{z_0}$ does not depend on the amplitude of the signal, as can be seen from Eqs. (28) and (30). This is no longer the case when the small-signal restriction $W \sim W_0$ is removed. Equation (16) was solved by numerical integration for various pulse shapes and amplitudes. The function below gives a simple fit to the computer plot, where h. s. pulse shapes are chosen to be unchirped:

$$\left.\frac{d\langle\dot{\varphi}\rangle}{dz}\right|_{z_0} = a(\Delta\omega_0, \tau)\,\frac{\kappa^2 W_0}{\eta c}\left(\frac{1-\cos\Theta}{\Theta^2}\right) \quad . \tag{32}$$

The dependence of $d\langle\dot{\varphi}\rangle/dz|_{z_0}$ on other pulse shapes is more complicated. No analytic fit was found for the general function $a(\Delta\omega_0, \tau)$, nor could we derive analytically the Θ dependence of (32) from Eq. (16). The oscillations of $d\langle\dot{\varphi}\rangle/dz|_{z_0}$ as a function of Θ become damped in the case of applied asymmetrical pulse shapes (Fig. 9). The periodicity in the integer $n(\Theta = 2n\pi)$ which holds in Eq. (23) has disappeared in the case of a doubly humped pulse (Fig. 10).

The frequency pushing for unchirped-input h. s. -shaped pulses of area π was calculated for a Gaussian and a Lorentzian line at various values of $\Delta\omega_0$ off resonance, and plotted as a function of the pulse width in Fig. 11. The general behavior of the curves agrees qualitatively well with the case of a Gaussian pulse given by Eq. (30).

C. Influence of Initial Chirp

As shown in Figs. 12 and 13, the magnitude of $d\langle\dot{\varphi}\rangle/dz$ at $z = z_0$ is strongly affected if initial phase modulation $\dot{\varphi}(z_0, t)$ or chirp exists in the applied pulse. The general behavior of the curves can be understood in terms of the weak-pulse approxima-

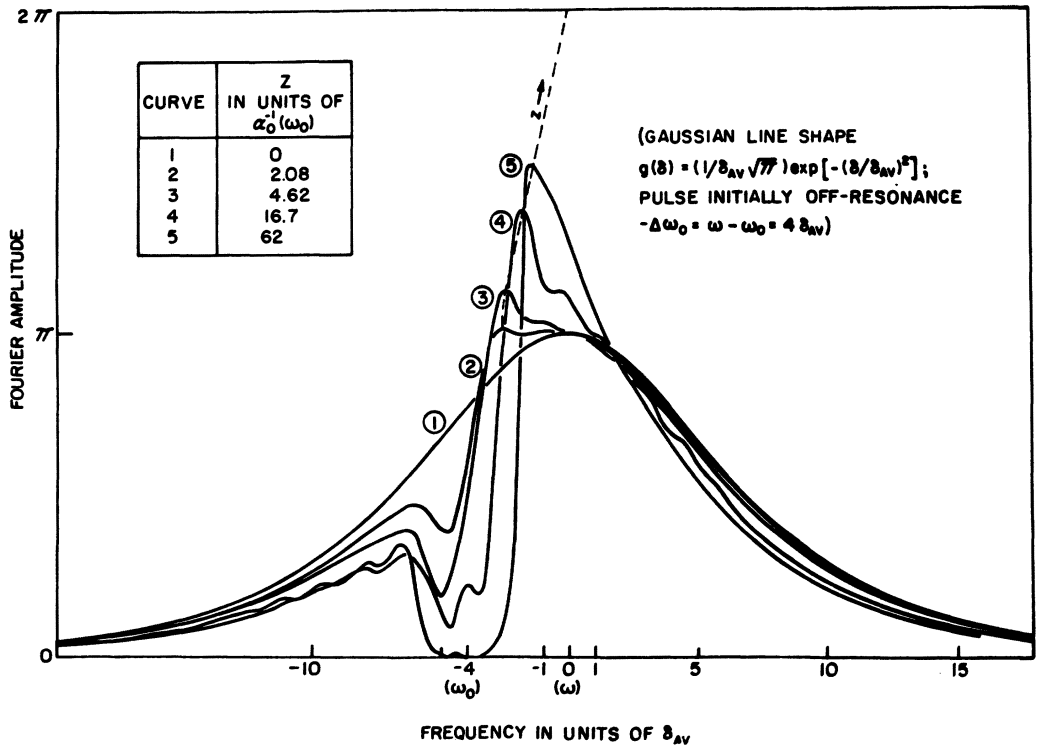

FIG. 6. Propagation of a pulse (initially four linewidths above resonance) through a Gaussian-broadened medium. The Fourier amplitude spectra are shown for five propagation-distance points. The initial pulse (1) is unchirped and h. s. shaped [initial pulse shape: sech($t/0.12$)].

tion applied in Sec. III B. For a given $\Delta\omega_0$ off resonance, Eq. (28) shows the frequency pushing is maximum if the pulse spectrum has a peak at the line frequency. This occurs for the phase amplitude parameter $a \approx \pm 3$ in Fig. 12. For $a = 0$, frequency pushing is a minimum. With initial chirp, these cases show that $d\langle\dot{\varphi}\rangle/dz$ is always of the same sign, signifying frequency pushing (with $T_2 = \infty$). This is in contrast to the results of Figs. 7 and 8, where the sign of $d\langle\dot{\varphi}\rangle/dz$ is seen to change during propagation, when no initial chirp is present. The choice of symmetry of the pulse modulation function $\varphi(t)$ relative to the pulse envelope function $\mathcal{E}(t)$ is critical in determining the nature of $d\langle\dot{\varphi}\rangle/dz$. If $\varphi(t)$ is in advance of $\mathcal{E}(t)$, it is strongly affected, as shown in Fig. 14. In the case of Fig. 15, $d\langle\dot{\varphi}\rangle/dz$ is shown to reverse sign.

Computer plots, similar to those shown in Figs. 2 and 3 for no initial chirp, show that self-induced transparency will occur in spite of the presence of

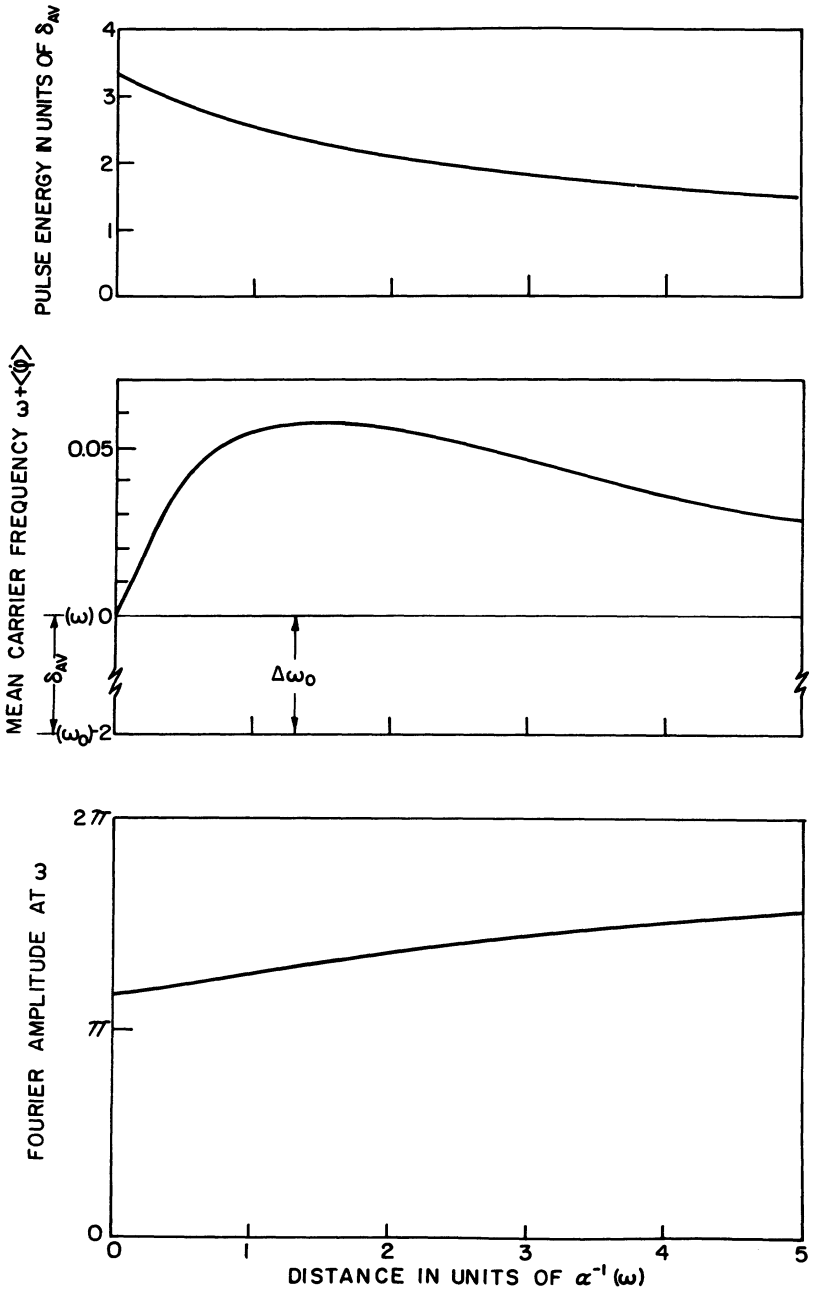

FIG. 7. Pulse energy, mean carrier frequency, and Fourier amplitude (at ω) as a function of propagation distance for the case shown in Fig. 2. [Lorentz line shape $g(\delta) = \delta_{AV}/\pi(\delta_{AV}^2 + \delta^2)$; pulse initially off-resonance $-\Delta\omega_0 = \omega - \omega_0 = 2\delta_{AV}$.]

initial chirp. Figures 16 and 17 show the evolution of an applied chirped pulse with its average frequency at exact resonance ω_0. It is remarkable that the chirped pulse remains at resonance. For this to occur, the function $\Delta W(\delta)$ must be an even function of δ for all symmetrically chirped pulses at resonance. We could not prove this property analytically, but accurate computer calculations of this function for h. s. -shaped pulses with Gaussian phase modulation at exact resonance showed that $\Delta W(\delta)$ was indeed an even function of δ. In the case of a symmetrically chirped pulse off resonance, a 2π h. s. pulse ultimately is formed at frequency ω. As in the case of off resonance, the chirped pulse at average frequency ω_0 splits into two parts with increasing z. The pulse portion earlier in time contains the enhanced phase modulation, while the later remaining pulse portion evolves toward a 2π h. s. pulse at the central line frequency. Compared with pulse modulation of the input pulse, the earlier pulse portion develops a much larger phase modulation with increasing distance. This is seen in terms of Fourier components which peak symmetrically about the resonance line, but overlap the wings of the resonance line spectrum only slightly. While the 2π h. s. pulse is expected to propagate without loss, the phase-modulated pulse will propagate with anomalously low loss. With increasing distance the Fourier component of the "fast" pulse at ω_0 approaches zero as the pulse modulation increases. The "fast" pulse is therefore attenuated at a slower rate, which is similar to the same effect which occurs in "zero-area" pulse propagation.[4]

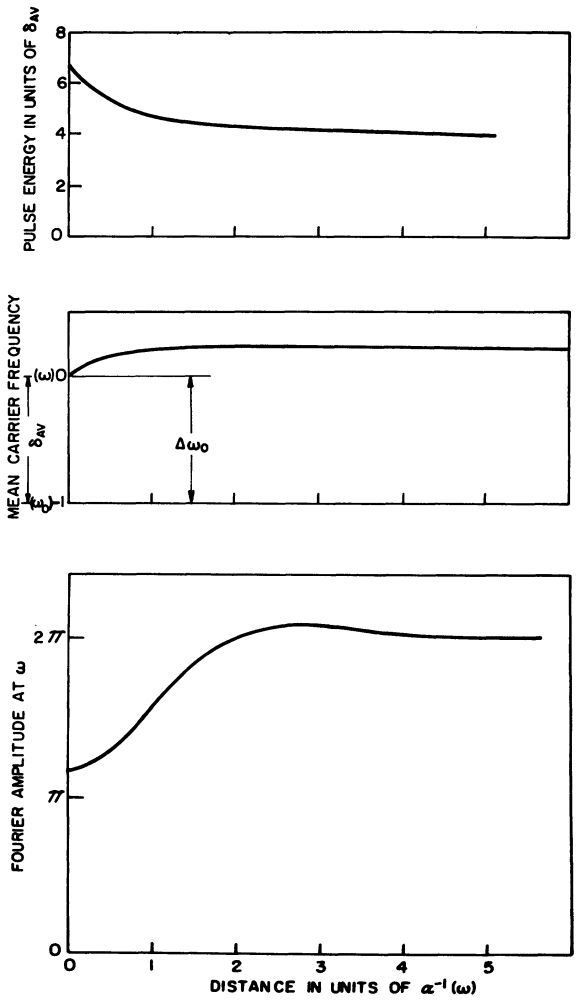

FIG. 8. Pulse energy, mean carrier frequency, and Fourier amplitude (at ω) as a function of propagation distance for the case shown in Fig. 3. [Gaussian line shape $g(\delta) = (1\delta_{AV}\sqrt{\pi})\exp[-(\delta/\delta_{AV})^2]$; pulse initially off resonance $-\Delta\omega_0 = \omega - \omega_0 = \delta_{AV}$].

We remind the reader that the area theorem[2]

$$\frac{d\Theta(z)}{dz} = -\frac{\alpha_0}{2}\sin\Theta(z) \quad , \tag{33}$$

with

$$\Theta(z) = \kappa \int_{-\infty}^{\infty} \mathcal{E}(z,t)\,dt \quad , \tag{34}$$

is invalid in the presence of continuous phase modulation. The linear absorption coefficient at resonance is defined as

$$\alpha_0 = \frac{8\pi\omega_0^2 p_0^2 N g(0)}{\eta\hbar c} \quad .$$

Equation (33) may be applied to the case of zero-area input $\Theta(0) = 0$ if the carrier is always nominally at constant frequency ω_0, but subjected to a sudden phase shift of π at $z = 0$, so that $\Theta(0) = \Theta(z) = 0$.

D. Off-Resonance Threshold for SIT

The process of phase modulation for a propagating pulse initially applied off resonance is inevitable (unless it is initially a 2π h. s. pulse) during its evolution toward a 2π h. s. pulse. In this case the question remains as to what the initial threshold area $\Theta_t(0)$ should be, above which SIT will occur. In the on-resonance non-phase-modulated case, $\Theta_t(0) = \pi$. Off resonance, there is strong evidence that $\Theta_t(0) < \pi$ is allowed. Here $\Theta_t(0)$ is determined by pulse shape and the off-resonance parameter $\Delta\omega_0$, whereas there is no such depen-

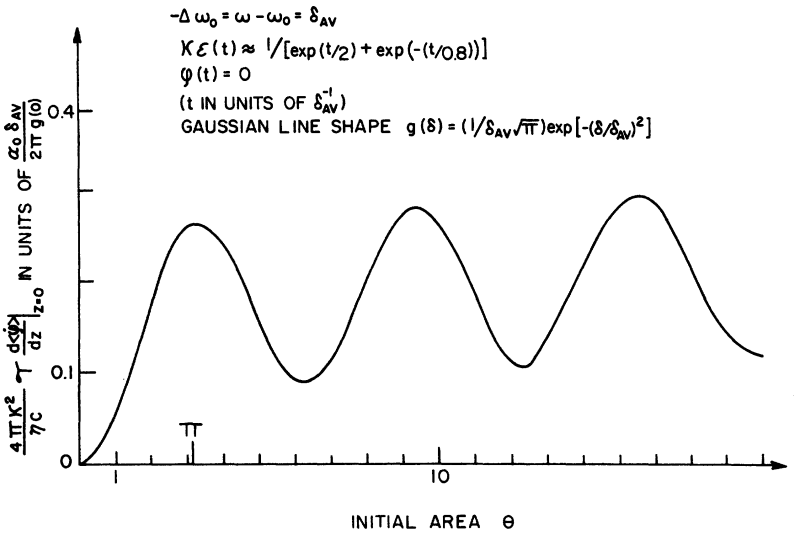

FIG. 9. Product of pulse energy and initial frequency pushing $d\langle\dot{\varphi}\rangle/dz\,|_{z_0}$ for an asymmetrical (unchirped) pulse, as a function of initial pulse area. In the case of a h. s. -shaped pulse of width 0.8, the corresponding graph would be the function

$$0.35\times(1-\cos\Theta)=\frac{4\pi\kappa^2}{\eta_c}\left.\frac{\langle d\dot{\varphi}\rangle}{dz}\right|_{z=0},$$

which relates to Eq. (32).

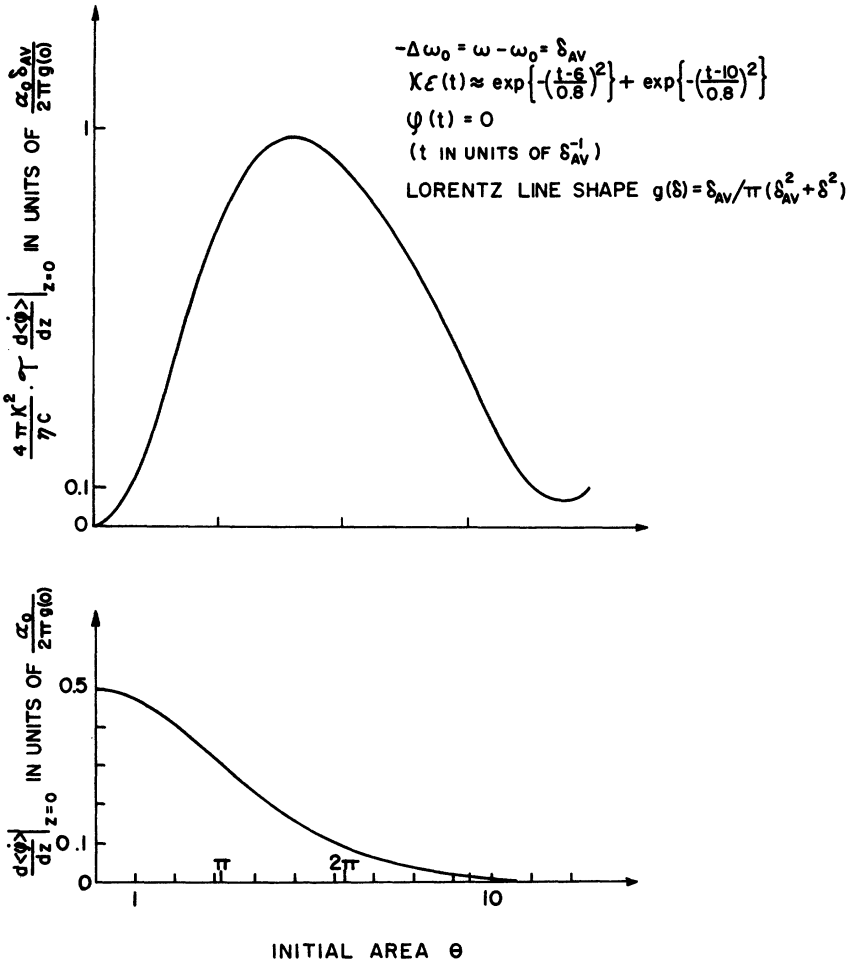

FIG. 10. Product of pulse energy and initial frequency pushing vs Θ(top). Initial frequency pushing vs Θ (bottom). Both plots apply to a double-peaked input pulse.

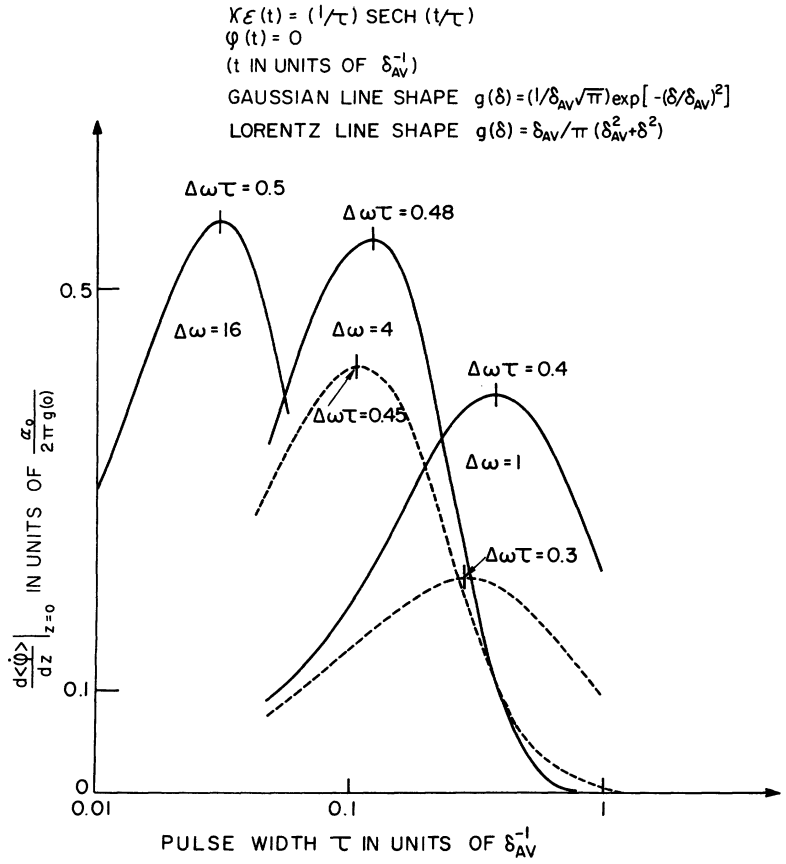

FIG. 11. Initial frequency pushing for input h. s. -shaped π pulses (unchirped) as a function of the amount off resonance ($\Delta\omega_0$) and pulse width (τ). The value of the product $\Delta\omega_0\tau$ is indicated.

dence for the on-resonance case.

Integration of Eq. (11) yields

$$\frac{d\Theta}{dz} = -\frac{2\pi\omega}{\eta c}\int_{-\infty}^{\infty} dt \int_{-\infty}^{\infty} v(\delta, z, t)g(\delta)\,d\delta \quad . \qquad (35)$$

Figure 18 plots numerical values of $d\Theta/dz$ from Eq. (35) for increasing values of Θ, but with the restriction that the pulses are always h. s. functions in shape. Care was taken to define correctly the phase and frequency of the polarization at the end of the pulse, where the dipoles begin to radiate at their natural frequencies. The first intersection of the $d\Theta/dz$ function versus Θ with positive slope at $d\Theta/dz = 0$ gives the value of $\Theta_f(0)$. Other pulse shapes give similar results, indicating that $\Theta_f(0) < \pi$. Allowing for naturally changing pulse shape may or may not contradict this behavior. However, the validity of $\Theta_f(0) < \pi$ behavior is favored from evidence given by the computer plots of Figs. 6 and 19, where changing pulse shape is taken into account. Figure 6 shows the change in Fourier spectrum versus specific z values for $\Theta(0) = 0.99\pi$, and Fig. 19 shows a similar behavior for $\Theta(0) = 2$. The peak of the Fourier transform increases monotonically with distance, and particularly at

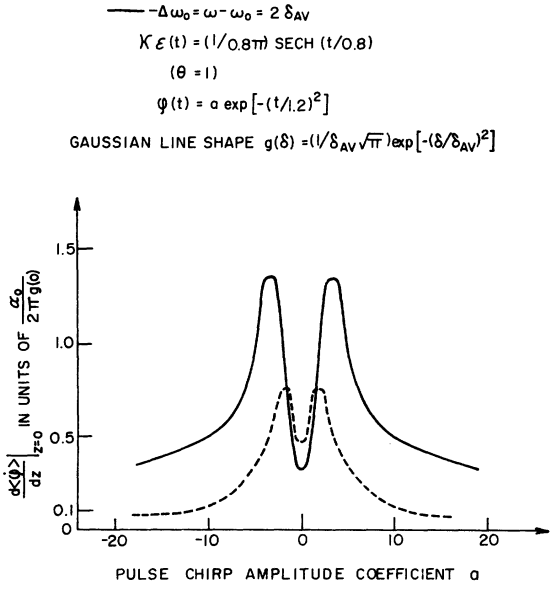

FIG. 12. Initial frequency pushing for a symmetrically chirped pulse off resonance, as a function of the amplitude (a) of the chirp. The resonance line is Gaussian broadened.

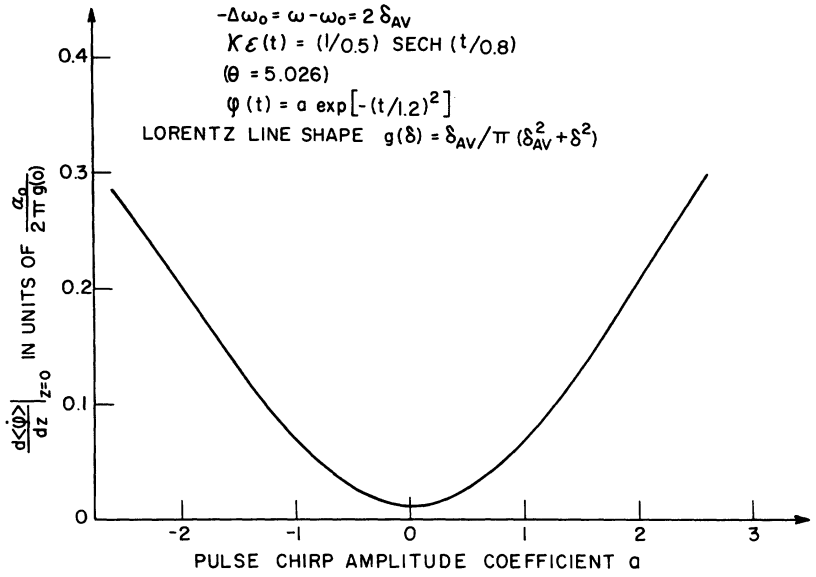

FIG. 13. Initial frequency pushing for a symmetrically chirped pulse off resonance, as a function of the amplitude (a) of the chirp. The resonance line is Lorentz broadened.

a very low rate for large $\Delta\omega_0$. The computer plots show that $\Theta_t(0) < \pi$ only occurs for input pulse widths $\tau < (\delta_{AV})^{-1} \sim T_2^*$.

IV. CASE OF AN EMITTER

A. Computer Results with Inhomogeneous Broadening

The choice of a plus sign in the definition of $W(\delta)$ in (14) corresponds to an amplifier. Therefore $\Delta W(\delta)$ is negative and finite for all z in Eq. (16). For $T_2 = \infty$, $\sigma = 0$, and specified initial conditions off resonance, computer plots in Figs. 20–22 show, respectively, $\langle\dot{\varphi}(z)\rangle$ versus z, $\mathcal{E}(z,t)$ and $\varphi(z,t)$ versus t for specific values of increasing z, and $\bar{\mathcal{E}}(\Omega, z)$ versus Ω for specific values of increasing z. As dictated by positive $d\langle\dot{\varphi}\rangle/dz$ from Eq. (16), Fig. 20 shows that $\omega + \langle\dot{\varphi}(z)\rangle$ approaches ω_0 with increasing propagation distance. The $\mathcal{E}(z,t)$ envelope develops oscillations during the approach, and the Fourier transforms $\bar{\mathcal{E}}(\Omega, z)$

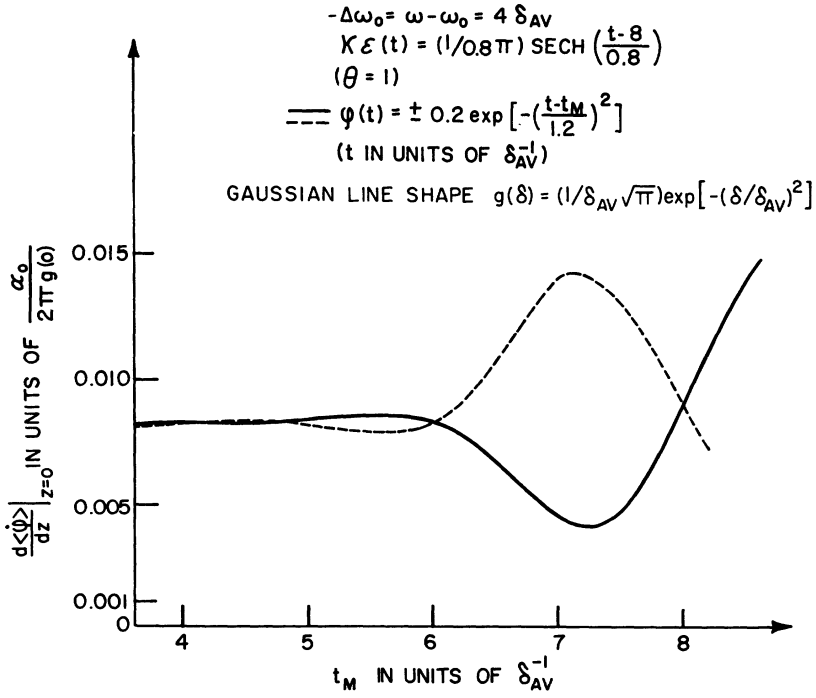

FIG. 14. Initial frequency pushing for an asymmetrically chirped pulse off resonance, as a function of the time position t_M of the chirp function $\varphi(t, t_M)$ with the amplitude of envelope $\mathcal{E}$ centered at $t = 8$; the case of a symmetrical pulse chirp corresponds to $t_M = 8$. The line broadening is Gaussian.

show the development of bumps on either side of $\omega+\langle\dot{\varphi}(z)\rangle$. At $d\langle\dot{\varphi}\rangle/dz=0$ for large z, it can be postulated from (16) that $\langle\dot{\varphi}\rangle=\Delta\omega_0$ if $\Delta W(\delta,z)$ and $g(\delta)$ are even functions of δ, or if $\delta=0$ (sharp-line case, no inhomogeneous broadening). This on-resonance pulling effect, accompanied by complete disappearance of phase modulation $\ddot{\varphi}(t,z\to\infty)=0$ at $\langle\dot{\varphi}\rangle=\Delta\omega_0$, has been confirmed by Hopf[5] in a computer analysis of the inhomogeneous-broadening case, taken up to large values of z. At the emitter resonance frequency the pulse is characterized by a Fourier amplitude of π at exact resonance, and by symmetric Fourier components[5,6] greater than π on either side of ω_0.

B. Steady-State Propagation

Although a form of equilibrium has been specified by $d\langle\dot{\varphi}\rangle/dz\to 0$ as $z\to\infty$ during propagation, there is an indefinite power increase

$$\frac{\eta c}{4\pi}\frac{d\mathcal{E}^2}{dz}>0 \ .$$

A scattering parameter σ is now included so that finite pulse energies $\mathcal{T}(z)$ may be reached. The case of homogeneous broadening is first considered. The equilibrium conditions to be applied to Eqs. (16) and (19) are as follows:

$$\frac{d\langle\dot{\varphi}^2\rangle}{dz}=\frac{d\langle\dot{\varphi}\rangle}{dz}=\frac{d\mathcal{T}}{dz}=\frac{d}{dz}\left(\frac{1}{\tau}\right)=0 \ , \tag{36}$$

$$\int_{-\infty}^{\infty}\frac{\partial\mathcal{E}^2}{dz}\,dt\to 0=\frac{-4\pi}{\eta c}\int_{-\infty}^{\infty}\omega v\mathcal{E}\,dt-\sigma\int_{-\infty}^{\infty}\mathcal{E}^2\,dt \tag{37}$$

or

$$\sigma\mathcal{T}=|\Delta W| \ ,$$

where $\omega\approx\omega_0$ with use of Eqs. (10) and (17). It follows that

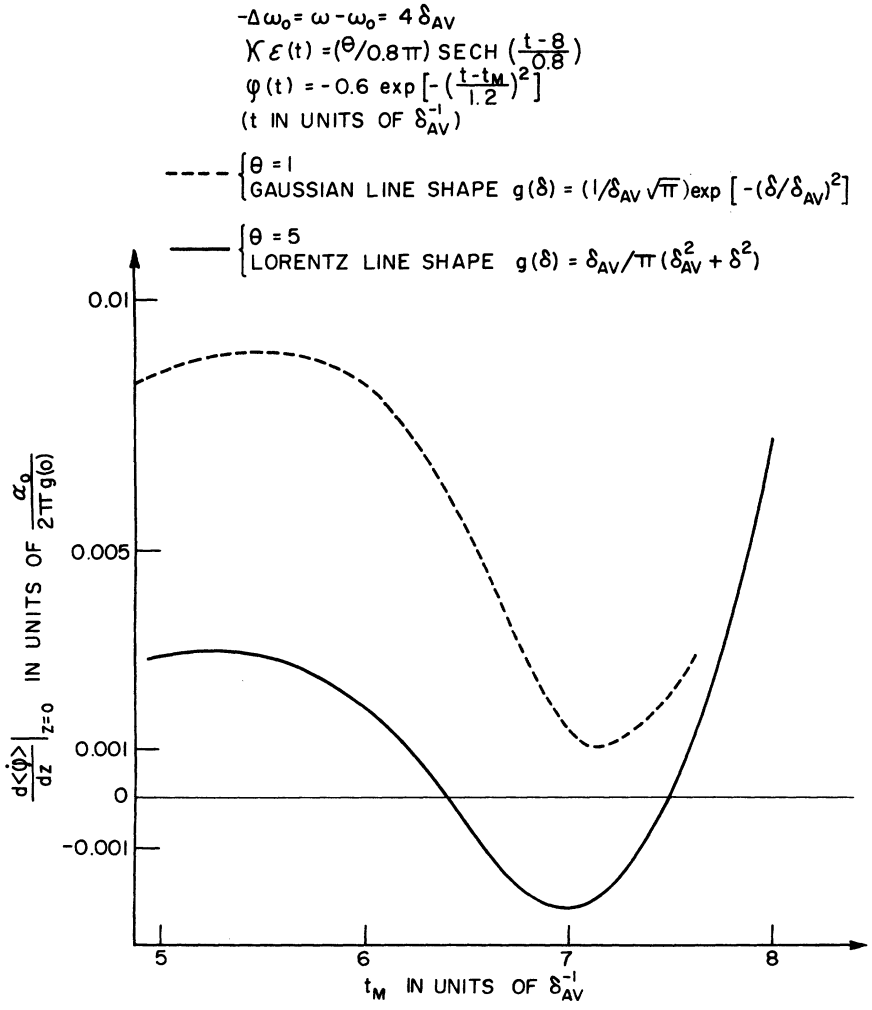

FIG. 15. Initial frequency pushing for asymmetrically chirped pulse off resonance, as a function of the time position t_M of the chirp function $\varphi(t,t_M)$ with the amplitude of envelope $\mathcal{E}$ centered at $t=8$; the case of a symmetrical pulse chirp corresponds to $t_M=8$. The line broadening is Lorentzian for $\Theta=5$ and Gaussian for $\Theta=1$, with $\varphi(t)$ common to both cases.

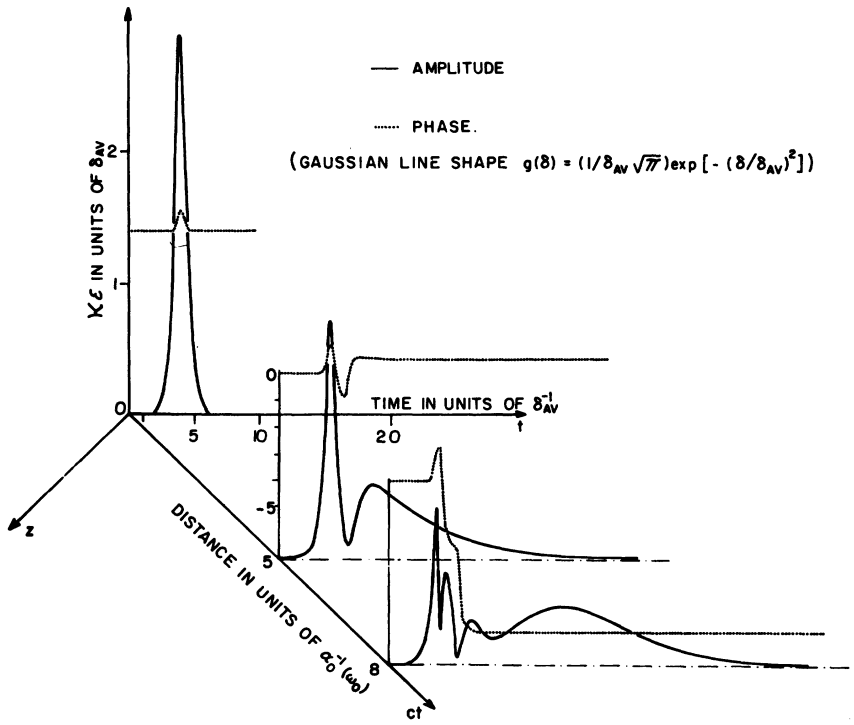

FIG. 16. Propagation of a chirped pulse at resonance through a medium which has Gaussian line broadening. The initial pulse area is $\Theta_0 = 3.64$. The initial pulse has h.s. envelope [sech$(t/0.4)$] and a Gaussian phase modulation [$\varphi(t) = 0.8\, e^{-t/0.42}$].

$$\frac{4\pi}{\eta c}\int_{-\infty}^{\infty} \dot{W}\mathcal{E}^2\,dt = -\sigma\int_{-\infty}^{\infty}\mathcal{E}^4\,dt\ . \tag{38}$$

After eliminating the term containing $\langle k'\rangle$ from (19) by using (16), and adding $-\langle\dot{\varphi}\rangle^2$ to both sides of (19), the equilibrium condition is found to be

$$q = \langle\dot{\varphi}^2\rangle - \langle\dot{\varphi}\rangle^2 = -\left(\frac{1}{\tau^2} + \frac{1}{T_2^2} + (\Delta\omega_0 - \langle\dot{\varphi}\rangle)^2\right) + \frac{\kappa^2}{\sigma\mathcal{T}}\int_{-\infty}^{\infty} dt\,\mathcal{E}^2\left(\frac{W}{T_2} - \frac{\dot{W}}{2}\right). \tag{39}$$

The mean-square frequency deviation is defined only for $q \geq 0$. For the medium gain to compensate scattering losses, the weighted averages of W and $-\dot{W}$ over $\mathcal{E}^2$ must be net positive.

If $q > 0$, chirping is defined as possible if the pulse intensity $\mathcal{E}^2$ is sufficiently large that the integral in (39) will dominate as a positive term, to make the right-hand side of (39) net positive. The condition (39) would also allow the existence of two or more pulses or of complex pulse shapes, and yet permit that widely differing spectral frequencies should average together to give $q > 0$. The term $1/\tau^2$ can be replaced by the more general expression given by (7).

If $q = 0$, then $\langle\dot{\varphi}^2\rangle = \langle\dot{\varphi}\rangle^2$, and there is no frequency modulation. Applying (38) to (39) to eliminate $\dot{W}$, and defining the mean field intensity

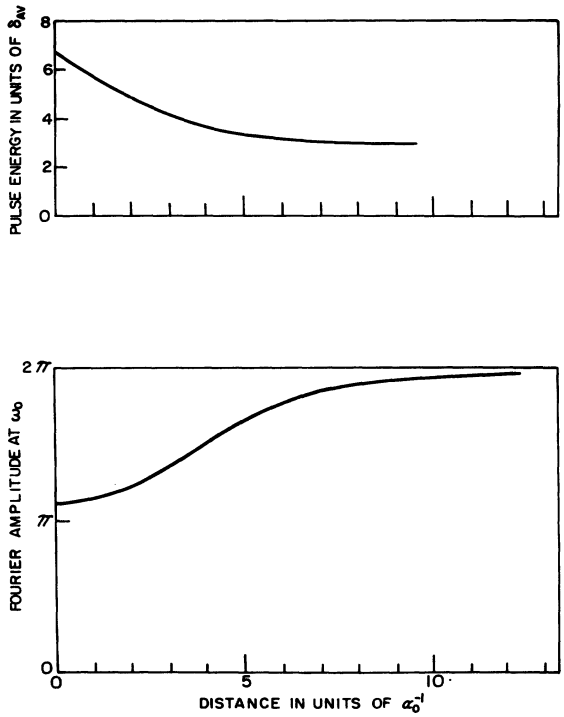

FIG. 17. Pulse energy and pulse area (defined here as the Fourier amplitude at resonance) as a function of propagation distance, for the case presented in Fig. 16. (Gaussian line shape $g(\delta) = (1/\delta_{AV}\sqrt{\pi})\exp[-(\delta/\delta_{AV})^2]$).

$$\langle \mathcal{E}^2 \rangle = \frac{\int_{-\infty}^{\infty} \mathcal{E}^4\, dt}{\int_{-\infty}^{\infty} \mathcal{E}^2\, dt} \quad ,$$

(39) reduces to

$$\frac{\kappa^2 \langle \mathcal{E}^2 \rangle}{2} + \frac{\kappa^2}{\sigma' T_2} \int_{-\infty}^{\infty} \mathcal{E}^2\, W\, dt = \frac{1}{\tau^2} + \frac{1}{T_2^2} . \qquad (40)$$

Previous investigators[7] have obtained a steady-state π h. s. pulse envelope solution which satisfies (40), and propagates at wave velocity $V_w = \eta/c$. The pulse envelope is given by

$$\mathcal{E} = \frac{1}{\kappa \tau_0} \operatorname{sech} \frac{t'}{\tau_0} \qquad (41)$$

and

$$W = W_0 \sigma' \left(\frac{1}{T_2} - \frac{1}{\tau_0} \tanh \frac{t'}{\tau_0} \right) \quad , \qquad (42)$$

where

$$\frac{1}{\tau_0} = \frac{1}{\sigma'} \left(1 - \frac{\sigma'}{T_2} \right) \quad ,$$

$$\tau_0 = \frac{\tau}{\sqrt{3}} \quad , \quad \sigma' = \frac{\sigma}{\alpha_0} T_2 \quad , \quad t' = t - z \frac{\eta}{c} \quad , \qquad (43)$$

$$\alpha_0 = \frac{4\pi \kappa^2 W_0 T_2}{\eta c} \quad ,$$

where α_0 is the linear absorption coefficient at resonance for a homogeneously broadened line.

We note that if (41) is substituted into Eq. (16) as an initial pulse under the assumption that the carrier is off resonance by a small amount $\Delta\omega_0$, the carrier frequency will pull toward ω_0 during its rise time, provided that $\sigma < 8\alpha_0/(8 + \pi^2)$. This is a condition for phase stability if a π pulse is to appear at exact resonance. It is independent of small $\Delta\omega_0$ because the frequency-pushing and -pulling terms in (16) are then each proportional to $\Delta\omega_0$, which cancels out. The stability test applies for initial $\dot{\varphi} = 0$ and for $-\infty \leq t \leq 0$. The condition for initial amplification of the input pulse is specified only by $\sigma < \alpha$.

In Appendix C steady-state conditions for pulse propagation in the emitter case are presented without the use of time averages. Wave and pulse velocities must remain constant for all z and t. In the case of pure homogeneous broadening, if the wave velocity is to be fixed at $V_w = c/\eta$, there can be no chirping and the carrier must be at resonance ($\Delta\omega_0 = \dot{\varphi}$). From the phase factor of Eq. (1), the wave velocity is defined as

$$V_w = \frac{\omega + \dot{\varphi}}{k - (\partial\varphi/\partial z)} \qquad (44)$$

at z and t. Therefore at equilibrium if

$$V_w = \frac{\eta}{c} = \frac{\omega_0}{k} \quad ,$$

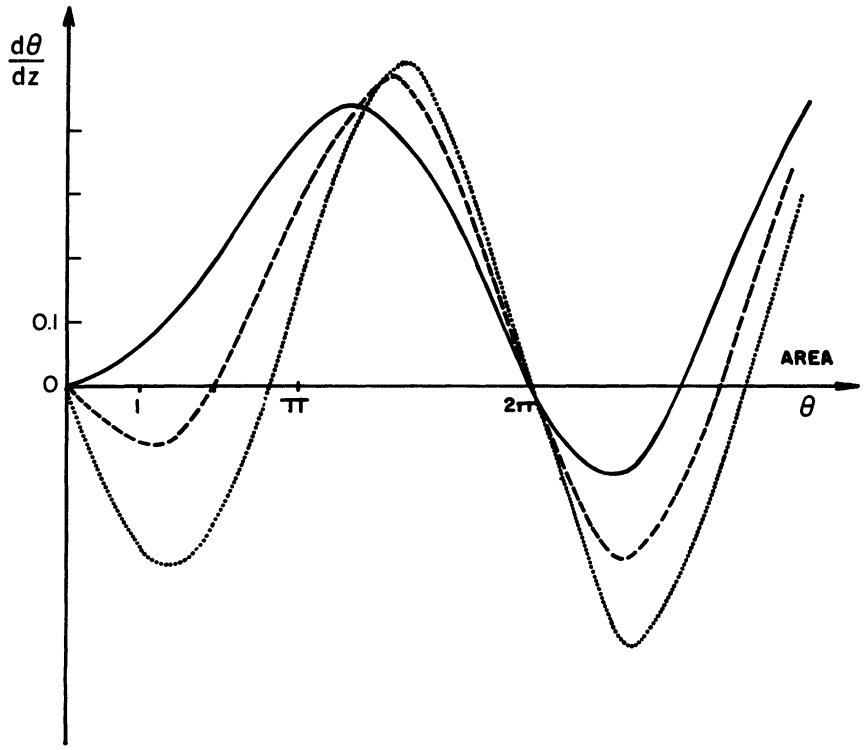

FIG. 18. Initial area increase $d\Theta/dz$ as a function of Θ for various amounts off resonance. The input-pulse shape is sech$(t/0.12)$ (unchirped). The line broadening is Gaussian. The amounts off resonance are two linewidths: $2\delta_{AV}$—dotted curve; three linewidths: $3\delta_{AV}$—dashed curve; four linewidths: $4\delta_{AV}$—solid curve. $d\Theta/dz$ is in units of $\delta_{AV}^{-1}\, \alpha_0/2\pi g(0)$.

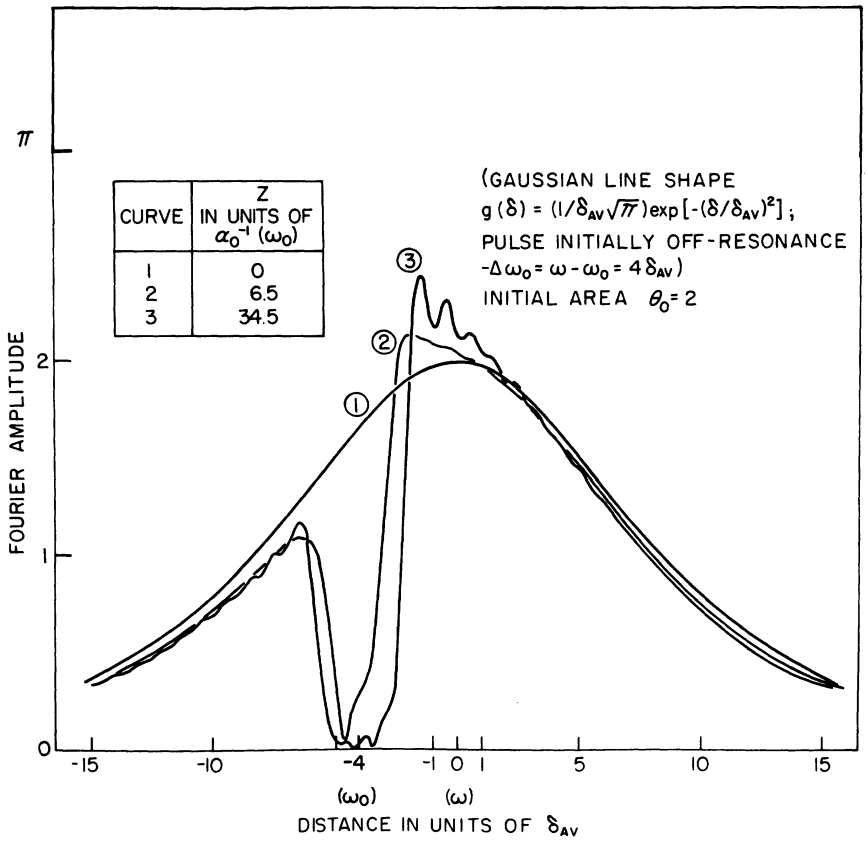

FIG. 19. Propagation of a pulse (initially four linewidths above resonance) through a Gaussian-braodened medium. The initial pulse has area 2, is unchirped, and is h.s. shaped [initial pulse shape: sech $(t/0.1)$]. The Fourier-amplitude spectra are shown for three propagation-distance points.

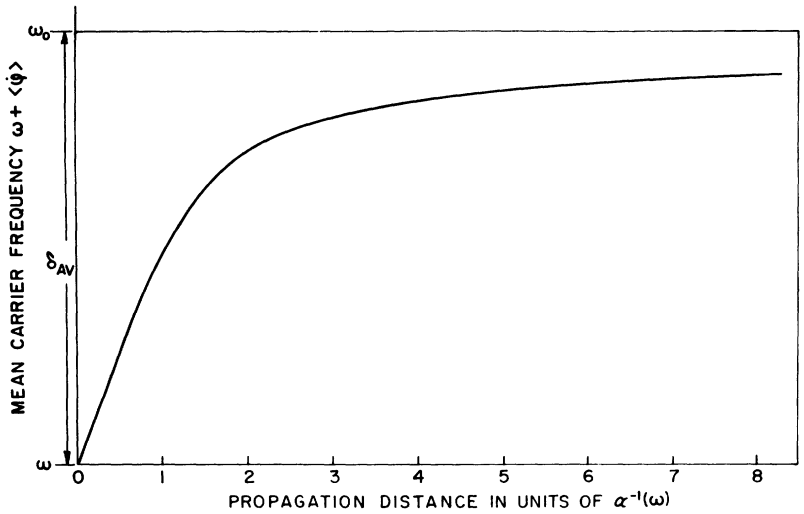

FIG. 20. Propagation of a pulse through an inhomogeneously broadened amplifier showing mean carrier frequency vs distance. The line broadening is Gaussian. The initial pulse is h.s. shaped [sech$(t/0.8)$], of area 0.5, and one linewidth ($\delta_{A.}$) below resonance.

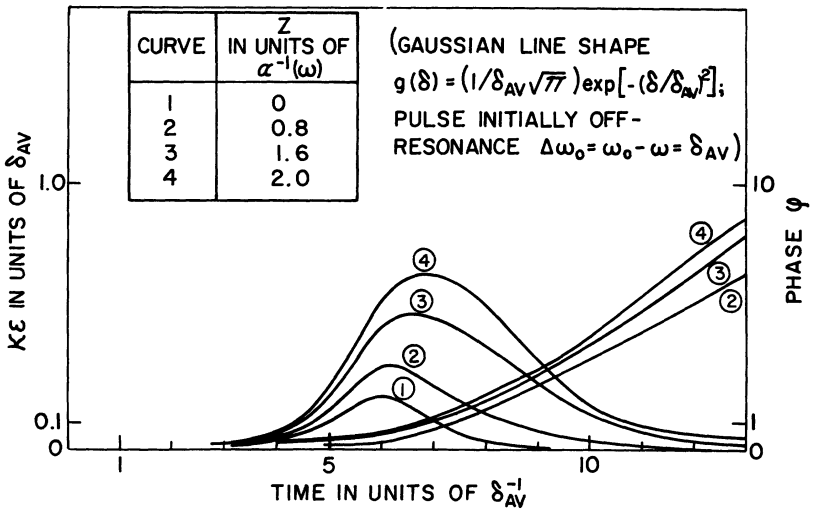

FIG. 21. Pulse shape and phase modulation as a function of propagation distance, for the case of Fig. 20, at four distance values. Field amplitude $\mathcal{E}$ and phase φ vs time.

then $\partial\varphi/\partial z = 0$ must hold at resonance. The slight change in η due to host-medium dispersion is neglected. If

$$V_w \neq \frac{\omega_0}{k} = \text{const}$$

is allowed, the existence of chirp is possible within the restrictions imposed by Eqs. (C1) and (C2) in Appendix C, applicable only to the case of homogeneous broadening. If inhomogeneous broadening is included together with homogeneous broadening, it is possible to have

$$V_w = \frac{\omega_0}{k} = \frac{\omega_0 + \dot{\varphi}}{k - (\partial\varphi/\partial z)} \quad ,$$

so that

$$\frac{k\dot{\varphi}}{\omega_0} = -\frac{\partial\varphi}{\partial z}$$

must be true at resonance. Now φ is no longer constant, but keeps track with the profile of the propagating pulse. In Appendix C it is shown in the case of pure homogeneous broadening, when $V_w = c/\eta(1 + c\sigma/\omega\eta)^{1/2} \neq c/\eta$, that a chirped steady-state solution exists for a pulse at a mean carrier frequency T_2^{-1} sec^{-1} above resonance.

For any existing chirp, the uncertainty relation $[\langle\Omega^2\rangle - \langle\dot{\varphi}\rangle^2]\tau^2 > 1$ would pertain to a pulse of width τ, where $\langle\Omega^2\rangle$ is defined in (6). The observed variation in pulse outputs of laser pulse outputs is usually attributed to the effect of nonliner changes in host-medium refractive index η, owing to high laser pulse powers, for example, from neodymium glass lasers. Our observations suggest that the nonlinear response of the two-level system itself might be a significant contributing factor.

C. Pulse Evolution with Homogeneous Broadening and $\sigma \neq 0$

Computer calculations show that the pulse carrier frequency in the emitter case approaches the

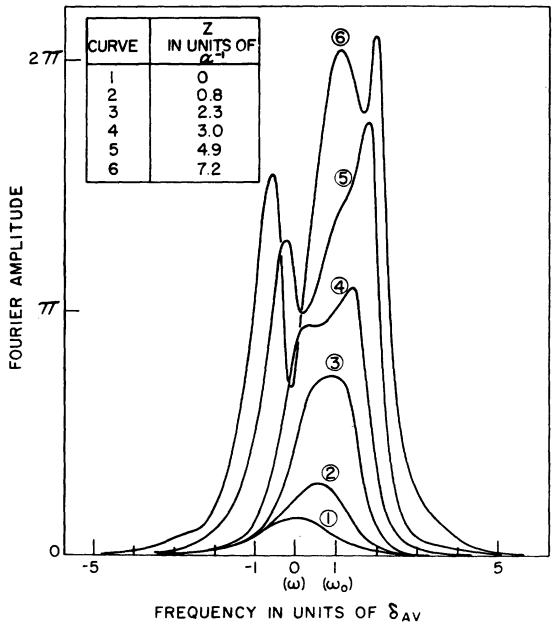

FIG. 22. Amplifier off-resonance: Fourier-amplitude spectra for six propagation distance. (Gaussian line shape $g(\delta) = (1/\delta_{AV}\sqrt{\pi})\exp[-(\delta/\delta_{AV})^2]$; pulse initially off resonance $\Delta\omega_0 = \omega_0 - \omega = \delta_{AV}$).

resonance at ω_0. We have chosen a few examples here which take into account scattering and incoherent damping parameters σ and T_2, but not inhomogeneous broadening ($\delta = 0$). According to the previous discussion, Fig. 23 shows what is expected typically. Here the pulse energy $\mathcal{T}(z)$ at $z \sim 10\alpha_0^{-1}$ begins a slow approach toward a constant value at $z = \infty$, while the carrier frequency slowly approaches ω_0. The shape of $\mathcal{E}(z,t)$ at the same time (not shown) approaches the π h.s. shape given by Eq. (41). Figure 24 demonstrates that an initially applied pulse of greater width (T_2 sec) exhibits a different history before the final slow approach begins. The pulse envelope and its Fourier transform are plotted in Figs. 25 and 26 for various propagation distances. Although the pulse ultimately approaches the solution of Eq. (41) at resonance, there is an initial approach and then recession of the carrier frequency towards and away from ω_0. A curious breakup into multiple pulse structure appears after the recession away from resonance. With the same pulse parameters used in Figs. 24–26 but applied off resonance by $T_2^{-1}/10$ instead, and with greater scattering loss, the pulse seems to stabilize over a longer distance in the off-resonance condition [and with shape and phase modulation quite different from the π h.s. solution of Eq. (41)]. For this case Fig. 27 shows $\mathcal{T}$ and $\Delta\omega_0 - \langle\dot{\varphi}\rangle$ versus z.

D. Effect of Higher-Order Terms on Pulse Propagation

For no scattering losses, the right-hand sides of Eqs. (11) and (12) indicate that significant changes in rates $\partial\mathcal{E}/\partial z$ and $\partial\varphi/\partial z$ are of the order

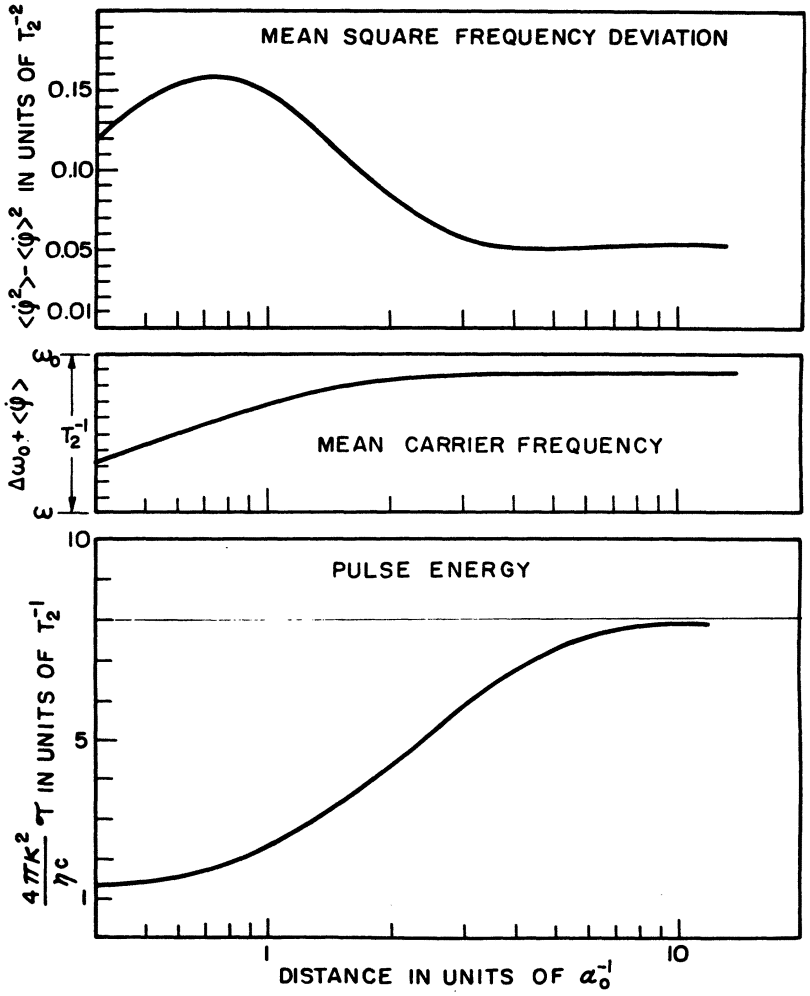

FIG. 23. Propagation of an initially short pulse through a homogeneously broadened amplifier. The mean-square deviations, the mean carrier frequency, and the pulse energy are plotted as a function of propagation distance. The h.s. π pulse expressed by Eq. (41) has an energy corresponding to $8T_2^{-1}$ for $z > 10\,\alpha_0^{-1}$. [$\Delta\omega_0 = \omega_0 - \omega = T_2^{-1}$; $\sigma = \alpha_0/5$; initial pulse shape $\kappa\mathcal{E}(t) = (T_2^{-1}/0.2\pi)\,\mathrm{sech}\,(t/0.2T_2)$].

of $\alpha(\omega)\mathcal{E}$ and $\varphi\alpha(\omega)$. Neglected higher-order rates are smaller by factors of $1/\omega T_2$, $(\Delta\omega/\omega)^2$, $\dot{\varphi}/\omega$, and $\kappa\mathcal{E}/\omega$, whichever is dominant. Our computer results show that steady-state pulses form in distances of order $\alpha^{-1}(\omega)$ in an absorber, and of the order of σ^{-1} in an emitter, taking $\sigma \ll \alpha$. The neglected higher-order terms would influence the "short-distance" steady-state pulses over extremely large distances of order $\omega T_2 \alpha^{-1}$, $(\omega/\Delta\omega_0)^2\alpha^{-1}$, $(\omega/\dot{\varphi})\alpha^{-1}$, or $(\omega/\kappa\mathcal{E})\alpha^{-1}$, whichever would be the shortest.

In the case of SIT, computer analysis shows that a 2π h. s. pulse is stable against small chirps and changes in shape. These perturbations are eliminated in distances of the order of $\alpha^{-1}(\omega)$. The effect of the higher-order terms is to shift the parameters of the 2π h. s. very slowly into parameters of another 2π h. s. pulse. As the pulse energy diminishes with propagation distance, the pulse width increases to maintain the pulse area $(\mathcal{E}_0\tau)$ a constant. The higher-order terms therefore cannot be the cause of exceedingly short or "preferred" pulse widths (even when the pulse is on resonance[8]) evolving from longer initial pulses. The tendency is instead for such pulses to become even longer instead of shorter because of losses.

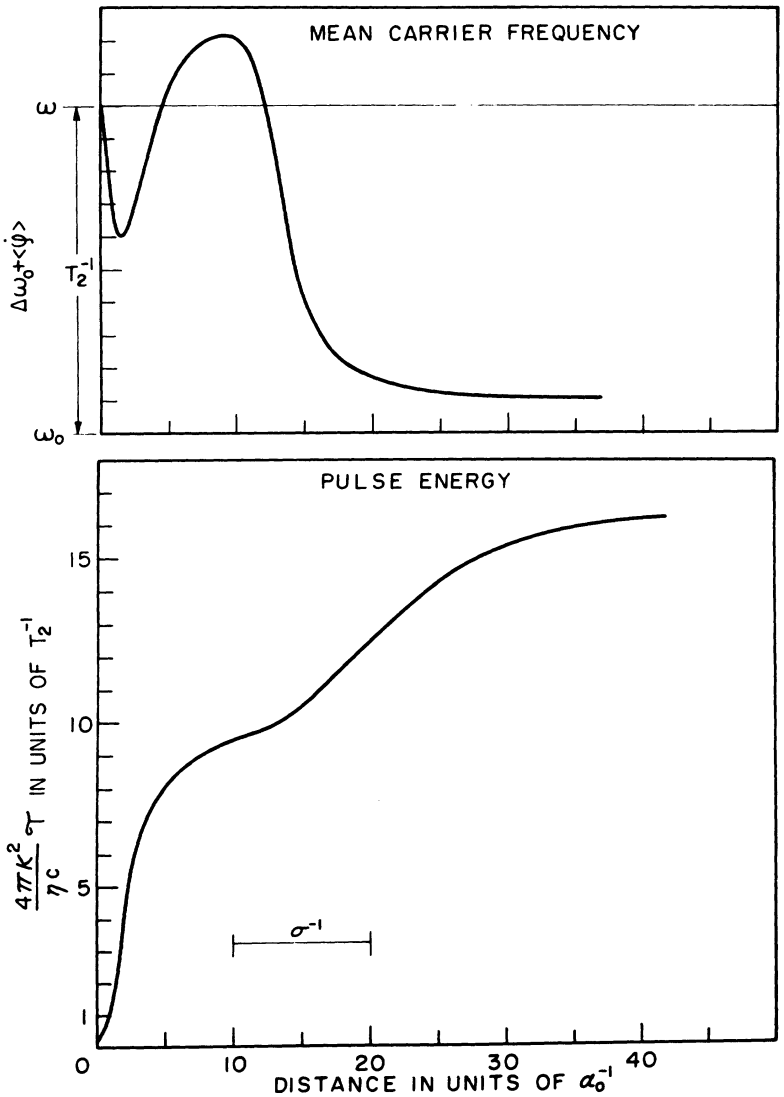

FIG. 24. Propagation of an initially long pulse through a homogeneously broadened amplifier. The mean carrier frequency and the pulse energy are plotted as a function of propagation distance. The h.s. π pulse expressed by Eq. (41) has an energy corresponding to $18T_2^{-1}$, for $z \gg 40\ \alpha_0^{-1}$. [$\Delta\omega_0 = \omega_0 - \omega = T_2^{-1}$; $\sigma = \alpha_0/10$; initial pulse shape $\kappa\mathcal{E}(t) = (T_2^{-1}/\pi)\ \mathrm{sech}\ (t/T_2)$.]

This argument applies as well to pulses of initially large area which break up into separate 2π h.s. pulses before the higher-order terms have effect after the pulse breakup.[2,9] As a given pulse width increases with propagation distance, it approaches the value of T_2 because of homogeneous broadening. At this point the pulse not only begins to be rapidly absorbed but also pulls in frequency towards resonance.[10]

V. CONCLUSIONS

A phenomenological and computer study is presented of the distance dependence of the carrier frequency of a pulse propagating through a two-level system for absorber and emitter cases under selected conditions of line broadening. The average frequency and spectral alterations of a single pulse show correlations with initial conditions of carrier phase modulation, where the average carrier frequency is initially on or off resonance. With only inhomogeneous broadening present, the average carrier frequency of a propagating pulse in an absorber initially pushes away from resonance. The pushing occurs at the greatest rate as a function of distance when the pulse is off resonance by an amount of the order of its inverse time width. Initial pulse areas in the vicinity of 2π or less show a breakup into two pulse groups with increasing distance of propagation. One of the pulses evolves toward a 2π h.s. pulse with slow pulse velocity, not phase modulated, while the other faster pulse decays away with a high degree of phase modulation, pushing progressively away from resonance. The net effect is that the average carrier frequency initially pushes away from resonance. After some distance of propagation the average frequency turns around and pulls toward resonance as the remaining 2π h.s. pulse takes shape, heading toward its original input carrier frequency. Therefore the ultimate formation of a 2π h.s. pulse off resonance requires a process of phase modulation during initial propagation. Associated with this process, computer calculations indicate that the threshold area for self-induced transparency is less than π, true only for short input pulses ($\tau < T_2^*$) applied initially off resonance. Experimental evidence in support of these computer results will be presented elsewhere.

In the case of an emitter, the pulse carrier is inevitably pulled to within the resonance line, which

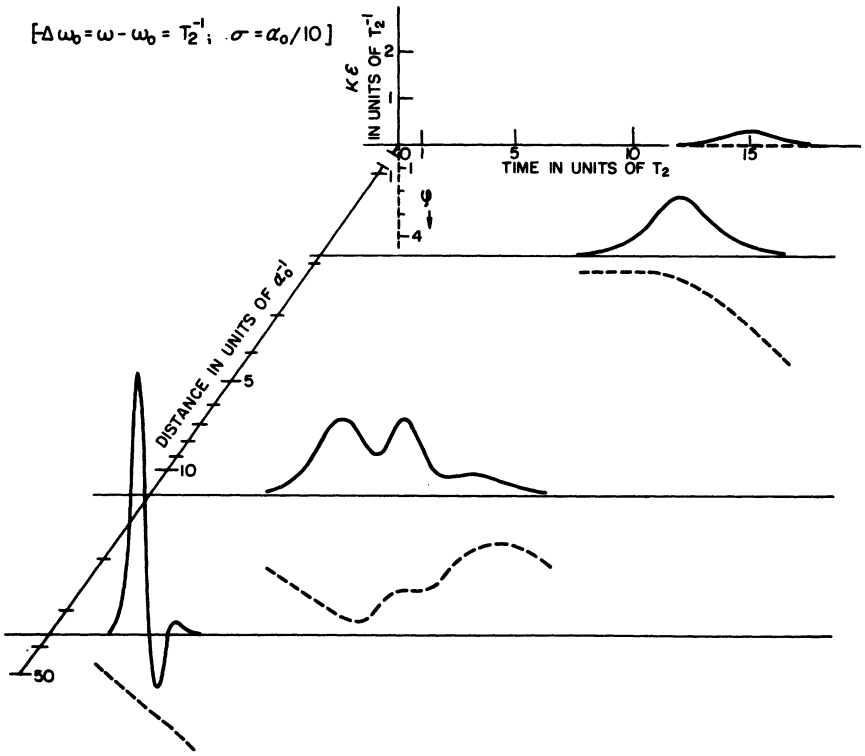

FIG. 25. Pulse envelope (amplitude $\kappa\mathcal{E}$ and phase φ) as a function of propagation distance for the case of Fig. 24.

is true also for a propagating continuous carrier wave. With damping present owing to homogeneous broadening, the average frequency may be temporarily pushed away from resonance over a finite distance. The pushing never occurs if the line is purely inhomogeneously broadened. A chirped pulse in steady state has been found analytically, without proof of uniqueness, to exist at an average frequency of one linewidth above resonance.

A description of average values of frequency modulation during pulse propagation is introduced in terms of first and second moments of frequency deviation of the pulse carrier frequency. Differential equations for the distance dependence of these moments are an aid in describing trends in pulse evolution and boundary conditions on pulse shape, dipole energy, pulse energy, and average carrier frequency. Our results are confined to an analysis of second-order phase-modulation effects which occur in the slowly-varying-envelope approximation. Backscattering is also neglected. It would appear that over long distances of propagation these neglected higher-order effects might become cumulative and therefore important. However, the average of cumulative first-order effects which we consider in the case of the emitter far exceed the neglected higher-order effects. The neglected higher-order effects are in a sense unimportant because they cannot become cumulative for an absorber and leave an imprint on propagating pulses. They result instead in irretrievable energy losses. We have shown from our computer results that a perturbation in shape or in phase modulation is eliminated from an input pulse, leading to a 2π h. s. pulse within "first-order distances." For long propagation distances one can say that the 2π h. s. shape is quasistationary, meaning that it slowly loses energy because of the higher-order terms. During this process the 2π area of the pulse remains essentially constant while the pulse width increases and the pulse amplitude decreases. In real physical situations, as the pulse width increases toward a value T_2, the pulse will then be rapidly absorbed. The propagation over extremely long distances does not allow for the existence of a stable pulse width associated with self-induced transparency.

ACKNOWLEDGMENTS

The authors wish to thank F. A. Hopf, S. L. McCall, M. O. Scully, J. H. Eberly, and T. M. Pierce for enlightening discussions.

APPENDIX A

In the text only incoherent damping caused by loss of phase memory is included by the T_2 time constant. The parameter T_2 may be considered to include effects of population changes in the levels

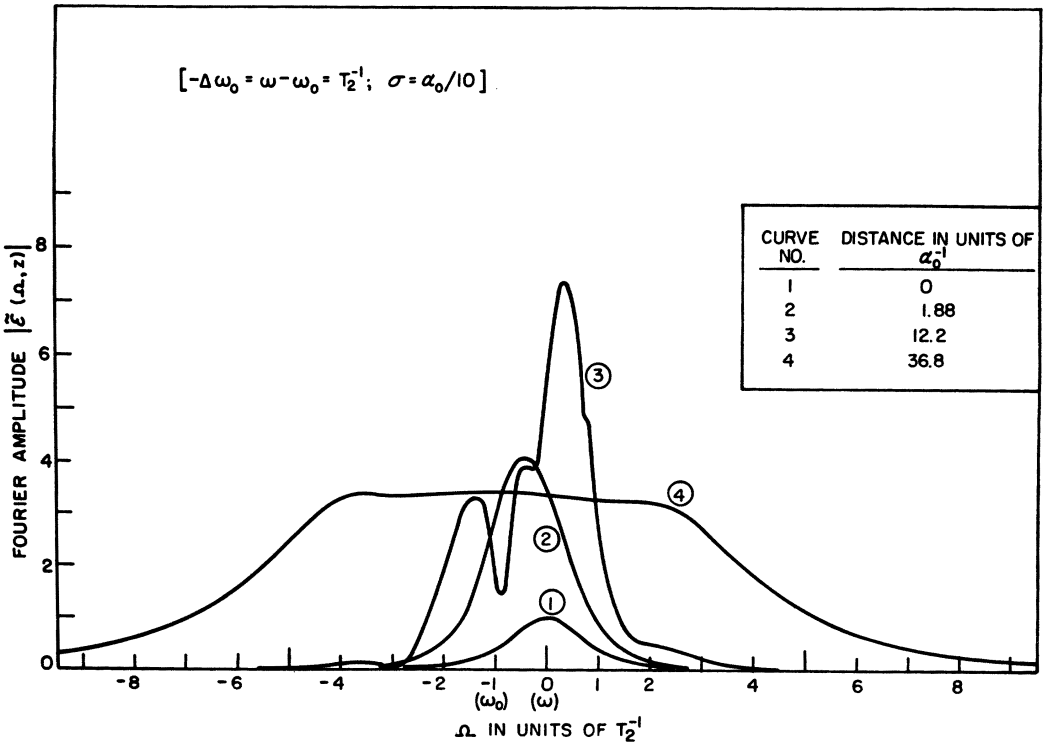

FIG. 26. Fourier plots at four distance points corresponding to the case of Figs. 24 and 25.

as well (i.e., spontaneous emission or collision effects) by introducing the relaxation-time constant T_1 into Eq. (10). Left by itself, the system would then approach the equilibrium internal energy W_0. Inclusion of some pumping mechanism allows the introduction of a pump term R, which replenishes the population of the excited state sufficiently to overcome the $1/T_1$ rate for decay to the ground state. Therefore Eq. (10) would be written

$$\dot{W} = \omega_0 \mathcal{E} v - \frac{W - W_0}{T_1} + R \ , \tag{A1}$$

where $W_0 = (\frac{1}{2}N)\hbar\omega_0 g(\delta)$ is the ground-state equilibrium energy. The initial energy of the two-level system at $t = -\infty$ would then be

$$W(\delta)\big|_{t=-\infty} = RT_1 - (\tfrac{1}{2}N)\hbar\omega_0 g(\delta) \ .$$

For the case of the emitter in our discussions we chose $RT_1 = N\hbar\omega_0 g(\delta)$, so that $W(\delta)|_{t=-\infty} = +|W_0(\delta)|$. During the action of a pulse over a short time τ, the effects of $1/T_1$ and R are considered negligible, and therefore are not included in Eq. (10).

Equations (11) and (12) are the slowly-varying-envelope approximations of the following wave equations:

$$\frac{\eta^2}{c^2}\frac{\partial^2 \mathcal{E}}{\partial t^2} - \frac{\partial^2 \mathcal{E}}{\partial z^2} + \mathcal{E}\left[\left(k - \frac{\partial \varphi}{\partial z}\right)^2 - \frac{\eta^2}{c^2}(\omega + \dot{\varphi})^2\right] = \frac{4\pi}{c^2}\int_{-\infty}^{\infty} [(\omega + \dot{\varphi})^2 u - 2(\omega + \dot{\varphi})\dot{v} - \ddot{\varphi} v - \ddot{u}] g(\delta)\, d\delta - \left(\frac{\eta\sigma}{c}\right)\dot{\mathcal{E}} \tag{A2}$$

and

$$\mathcal{E}\left(\frac{\eta^2}{c^2}\frac{\partial^2 \varphi}{\partial t^2} - \frac{\partial^2 \varphi}{\partial z^2}\right) + 2\left(k - \frac{\partial \varphi}{\partial z}\right)\frac{\partial \mathcal{E}}{\partial z} + \frac{2\eta^2}{c^2}(\omega + \dot{\varphi})\dot{\mathcal{E}} = -\frac{4\pi}{c^2}\int_{-\infty}^{\infty} [(\omega + \dot{\varphi})^2 v + 2(\omega + \dot{\varphi})\dot{u} + \ddot{\varphi} u - \ddot{v}] g(\delta)\, d\delta$$
$$- (\omega + \dot{\varphi})\frac{\eta\sigma}{c}\mathcal{E} \ . \tag{A3}$$

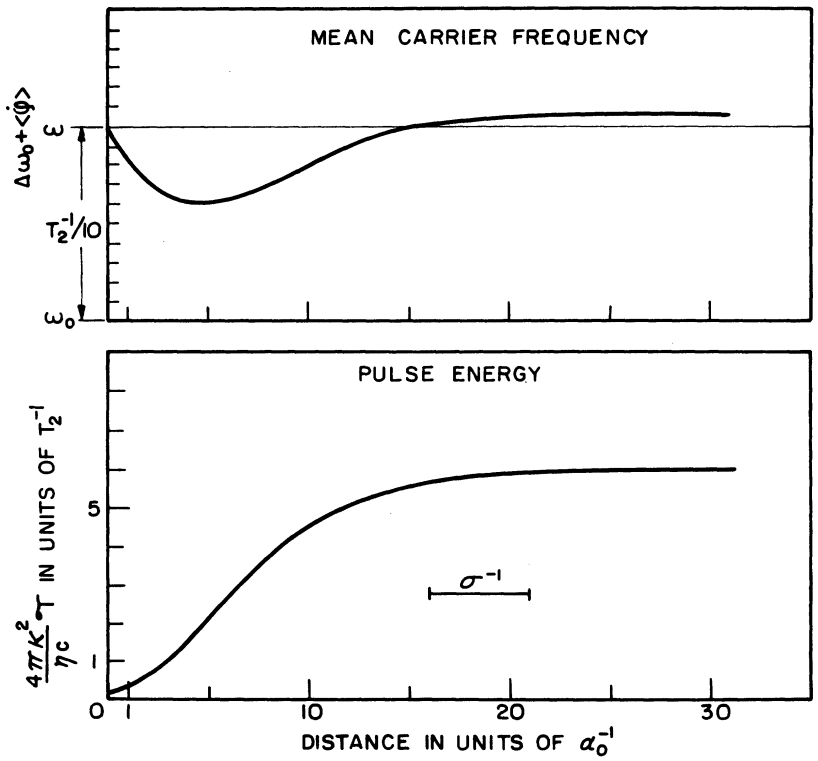

FIG. 27. Propagation of an initially long pulse through a homogeneously broadened amplifier. The same initial pulse is used as in Fig. 24, except that it is $T_2^{-1}/10$ sec^{-1} off resonance instead of T_2^{-1} sec^{-1}, and the scattering loss is doubled. The inverse pulse width remains large compared to $[(1/\sigma^1)\times(1-\sigma/T_2)]^{-1}$ [below Eq. (42)]. [$\Delta\omega_0 = \omega_0 - \omega = -T_2^{-1}/10$; $\sigma = \alpha_0/5$; initial pulse shape $\kappa\mathcal{E}(t) = (T_2^{-1}/\pi)\,\mathrm{sech}(t/T_2)$.]

Making use of the first two equations (8) and (9), in the approximation that

$$\frac{1}{\omega T_2}, \quad \frac{\kappa \mathcal{E}}{\omega}, \quad \frac{\varphi}{2\omega}, \quad \left(\frac{\Delta\omega}{\omega}\right)^2, \quad \frac{1}{\omega T_2^*}, \quad \frac{\ddot{\varphi}}{\omega^2}, \quad \frac{\ddot{u}}{\omega^2 u}, \quad \frac{\ddot{v}}{\omega^2 v}, \quad \left(\sigma / \frac{\partial \varphi}{\partial z}\right)\left(\frac{\mathcal{E}}{\omega \mathcal{E}}\right) \ll 1 ,$$

Eqs. (A2) and (A3) reduce to

$$\mathcal{E}\left(\frac{\partial \varphi}{\partial z} + \frac{\eta}{c}\dot{\varphi}\right) = -\frac{2\pi(\omega + 2\Delta\omega_0)}{\eta c}\int_{-\infty}^{\infty} u g(\delta)\, d\delta$$

and

$$\frac{\partial \mathcal{E}}{\partial z} + \frac{\eta}{c}\dot{\mathcal{E}} = -\frac{2\pi(\omega + 2\Delta\omega_0)}{\eta c}\int_{-\infty}^{\infty} v g(\delta)\, d\delta - \frac{\sigma \mathcal{E}}{2} .$$

APPENDIX B

Second-Moment Equation

The following derivation is carried out in the retarded-time frame.

From the definitions given by Eqs. (5) and (17) the following derivative is written:

$$\frac{d}{dz}\left(\mathcal{T}\langle\dot{\varphi}^2\rangle\right) = \frac{\eta c}{4\pi}\int_{-\infty}^{\infty} \dot{\varphi}^2 \frac{\partial \mathcal{E}^2}{\partial z}\, dt + \frac{\eta c}{4\pi}\int_{-\infty}^{\infty} \mathcal{E}^2 \frac{\partial \dot{\varphi}^2}{\partial z}\, dt . \tag{B1}$$

The first term on the right-hand side is

$$\frac{\eta c}{4\pi}\int_{-\infty}^{\infty} \dot{\varphi}^2 \frac{\partial \mathcal{E}^2}{\partial z}\, dt = -\sigma \mathcal{T}\langle\dot{\varphi}^2\rangle - \frac{\omega}{\omega_0}\int_{-\infty}^{\infty} dt \int_{-\infty}^{\infty} \dot{\varphi}^2 \dot{W} g(\delta)\, d\delta , \tag{B2}$$

using Eq. (11) with inclusion of the scattering term $-\frac{1}{2}(\sigma\mathcal{E})$. Using Eq. (12), the last term in (B1) is expressed as

$$\frac{\eta c}{2\pi}\int_{-\infty}^{\infty} \dot{\varphi}\frac{\partial \dot{\varphi}}{\partial z}\mathcal{E}^2\, dt = -\omega\int_{-\infty}^{\infty} dt \int_{-\infty}^{\infty} (\dot{\varphi} u \mathcal{E} - u\dot{\varphi}\dot{\mathcal{E}}) g(\delta)\, d\delta . \tag{B3}$$

For the second term of (B3), using Eq. (9) and integrating by parts gives

$$\omega\int_{-\infty}^{\infty} dt \int_{-\infty}^{\infty} (u\dot{\varphi})\dot{\mathcal{E}} g(\delta)\, d\delta = \omega\int_{-\infty}^{\infty} dt \int_{-\infty}^{\infty} \left(\dot{v} + \frac{\kappa^2 \mathcal{E} W}{\omega_0} + \Delta\omega u + \frac{v}{T_2}\right)\dot{\mathcal{E}} g(\delta)\, d\delta$$
$$= \omega\int_{-\infty}^{\infty} dt \int_{-\infty}^{\infty} \left(\dot{v}\dot{\mathcal{E}} + \frac{\kappa^2 \mathcal{E}\dot{\mathcal{E}} W}{\omega_0} + \frac{v\dot{\mathcal{E}}}{T_2} - \Delta\omega \dot{u}\mathcal{E}\right) g(\delta)\, d\delta . \tag{B4}$$

For the various terms of (B4), again using Eqs. (8)–(10) and integrating by parts, we have

$$-\omega\int_{-\infty}^{\infty} dt \int_{-\infty}^{\infty} \Delta\omega \dot{u}\mathcal{E} g(\delta)\, d\delta = -\int_{-\infty}^{\infty} dt \int_{-\infty}^{\infty} \left[\frac{\omega}{\omega_0}\Delta\omega(\Delta\omega - \dot{\varphi})\dot{W} - (\Delta\omega)\left(\omega \frac{u\mathcal{E}}{T_2}\right)\right] g(\delta)\, d\delta \tag{B5}$$

and

$$\omega\int_{-\infty}^{\infty} dt \int_{-\infty}^{\infty} \frac{v\dot{\mathcal{E}}}{T_2} g(\delta)\, d\delta = -\omega\int_{-\infty}^{\infty} dt \int_{-\infty}^{\infty} \frac{\dot{v}\mathcal{E}}{T_2} g(\delta)\, d\delta$$
$$= \frac{\omega}{T_2}\int_{-\infty}^{\infty} dt \int_{-\infty}^{\infty} \left(u\mathcal{E}(\Delta\omega - \dot{\varphi}) + \frac{\kappa^2 \mathcal{E}^2 W}{\omega_0} + \frac{\mathcal{E} v}{T_2}\right) g(\delta)\, d\delta . \tag{B6}$$

Introducing the definition of the pulse width given by Eq. (7) into Eq. (11), and taking into account the scattering term σ,

$$\frac{d}{dz}\left(\frac{\mathcal{T}}{\tau^2}\right) = \frac{\eta c}{4\pi}\frac{d}{dz}\int_{-\infty}^{\infty} \mathcal{E}^2\, dt = -\omega\int_{-\infty}^{\infty} dt \int_{-\infty}^{\infty} \dot{\mathcal{E}} v g(\delta)\, d\delta - \sigma\frac{\mathcal{T}}{\tau^2}$$

or

$$\omega\int_{-\infty}^{\infty} dt \int_{-\infty}^{\infty} \dot{\mathcal{E}} v g(\delta)\, d\delta = -\frac{d}{dz}\left(\frac{\mathcal{T}}{\tau^2}\right) - \sigma\left(\frac{\mathcal{T}}{\tau^2}\right) . \tag{B7}$$

And finally, we have

$$\cdot\int_{-\infty}^{\infty} dt \int_{-\infty}^{\infty} \kappa^2 \mathcal{E}\dot{\mathcal{E}} W g(\delta)\, d\delta = +\frac{1}{2}\int_{-\infty}^{\infty} dt \int_{-\infty}^{\infty} \kappa^2 W \frac{\partial \mathcal{E}^2}{\partial t} g(\delta)\, d\delta = -\frac{1}{2}\int_{-\infty}^{\infty} dt \int_{-\infty}^{\infty} \kappa^2 \mathcal{E}^2 \dot{W} g(\delta)\, d\delta \ . \tag{B8}$$

The relations (B5)–(B8) are introduced into (B4). Equations (B3) and (B2) are thus determined, which apply to (B1). After subtracting

$$\langle \dot{\varphi}^2 \rangle \frac{d\mathcal{T}}{dz} = -\sigma \langle \dot{\varphi}^2 \rangle - \frac{\omega}{\omega_0} \int_{-\infty}^{\infty} \langle \dot{\varphi} \rangle^2 \Delta W g(\delta)\, d\delta \tag{B9}$$

from (B1), Eq. (19) is the final result.

APPENDIX C

The wave velocity V_w defined by (44) is a constant velocity at which the phase modulation must also propagate if a steady-state pulse is to exist. From Eqs. (A2) and (A3) of Appendix A, retention of terms V_w and V_w^2 and dropping other higher-order terms gives the following equations:

$$\left(1 - \frac{\eta^2 V_w^2}{c^2}\right)\mathcal{E} = \frac{4\pi V_w^2}{c^2}\int_{-\infty}^{\infty} u g(\delta)\, d\delta \ , \tag{C1}$$

$$\frac{\partial \mathcal{E}}{\partial z} + \frac{\eta^2}{c^2} V_w \dot{\mathcal{E}} = -\frac{2\pi V_w}{c^2}\omega \int_{-\infty}^{\infty} v g(\delta)\, d\delta - \frac{n\sigma V_w}{2c}\mathcal{E}$$

$$= \left(-\frac{1}{V} + \frac{\eta^2}{c^2} V_w\right)\dot{\mathcal{E}} \ . \tag{C2}$$

These equations describe only the propagation in steady state. The term $-(1/V)\dot{\mathcal{E}}$ on the right-hand side of (C2) indicates that the envelope or "pulse velocity," given by V, is also a constant not necessarily the same as V_w in the absence of a chirp. The steady state would require $V = V_w$ if a chirp is present. A steady-state dispersion relation is found by combining (C1) and (C2) with Eq. (8):

$$\Delta\omega_0 - \dot{\varphi} = \frac{\gamma\omega}{2}\frac{p+1}{\gamma' p - \frac{1}{2}(\eta c\sigma T_2)} + \frac{2\pi\omega T_2 \int_{-\infty}^{\infty} v(\delta) g(\delta)\, d\delta}{\left[\gamma' p - \frac{1}{2}(\eta c\sigma T_2)\right]\mathcal{E}} .$$

Here

$$p = T_2 \frac{\dot{\mathcal{E}}}{\mathcal{E}} , \quad \gamma = \frac{c^2}{V_w^2}\left(1 - \frac{\eta^2 V_w^2}{c^2}\right),$$

$$\gamma' = \frac{c^2}{V_w^2}\left(\frac{V_w^2}{V^2} - \frac{\eta^2 V_w^2}{c^2}\right) \ . \tag{C3}$$

Equations (C1) and (C3) are consistent with the case of self-induced transparency, where $T_2 = \infty$ and $\sigma = 0$. In that case, where u is proportional to $\mathcal{E}$, and v is proportional to $\dot{\mathcal{E}}$, there is no chirp and $\ddot{\varphi} = 0$. Constant and arbitrary values of $\dot{\varphi}$, V, and V_w therefore exist for SIT according to the constraint imposed by (C3). For an amplifier (letting $\sigma \neq 0$) there can only be an unchirped solution at resonance ($\dot{\varphi} = \Delta\omega_0$) in the sharp-line limit for $V_w = c/\eta$ ($\gamma = 0$), while off resonance it would be chirped for $V_w \neq c/\eta$. The average frequency of the carrier is defined as ω for all t. With inhomogeneous and homogeneous broadening present simultaneously, chirping is generally possible within the constraint imposed by (C3) and Eq. (39), where $q \geq 0$. In a proof of the uniqueness of an on-resonance π pulse (inhomogeneous broadening absent), the possible dispersion of the resonant medium was excluded by assuming $V_w = c/\eta$ [Eqs. (19) and (38) of Ref. 7, Arrechi *et al.*], thus reducing its generality.

In the absence of inhomogeneous broadening, the combination of (C3) with (9) and (10) yields the following complicated equation:

$$p'' + \frac{p'^2}{p} + \frac{3p'}{\mathcal{E}} + \left(1 - \frac{\eta c\sigma T_2}{2\gamma}\right)\frac{p'}{p\mathcal{E}}$$
$$+ \kappa^2 T_2^2\left(p - \frac{\eta c\sigma T_2}{2\gamma}\right)\frac{1}{p^2}$$
$$- \frac{\gamma\omega^2 T_2^2}{2\eta c\sigma T_2}\left(\frac{p'}{p\mathcal{E}}\right)\frac{1}{[1 - (2\gamma/\eta c\sigma T_2)p]^2} = 0 \ . \tag{C4}$$

Here the relationships $V = V_w$ and $\gamma = \gamma'$ are applied. The π h.s. pulse expressed by Eq. (41) is a solution of (C4) for $V_w = c/\eta$ ($\gamma = 0$). In the approximation that $\omega T_2 \gg 1$ and $c\sigma\omega T_2\tau_0 \gg 1$, Eq. (C4) has a different solution, not proven unique, which is chirped, off resonance, and propagates with a velocity $V_w \neq c/\eta$. The following relations apply:

$$\mathcal{E}(t') = \frac{\sqrt{2}}{\kappa\tau_0}\operatorname{sech}\left(\frac{t'}{\tau_0}\right) ,$$

$$\Delta\omega_0 - \dot{\varphi} = -\frac{1}{T_2} + \frac{1}{\tau_0}\tanh\left(\frac{t'}{\tau_0}\right) ,$$

$$\omega = \omega_0 + \frac{1}{T_2} \ , \quad V_w = \frac{c}{\eta[1 + (\lambda\sigma/2\pi)]^{1/2}} \ , \tag{C5}$$

where

$$\lambda = \frac{2\pi c}{\eta\omega} \ , \quad 3\tau_0^2 = \tau^2 \ , \quad t' = t - \frac{z}{V_w} \ .$$

These solutions (C5) correspond to a $\pi\sqrt{2}$ pulse (the envelope area) symmetrically chirped, with carrier frequency centered at $\omega_0 + (1/T_2) = \omega$. It will be shown below [(C6)] that the pulse width is related to the density of resonant dipoles through W_0. Although $\tau_0 > T_2$ is allowed, there is an upper limit to the value of τ_0 set by the relationship $\mathcal{E} \propto (1/\tau_0)$, because $p_0\mathcal{E}$ must greatly exceed the dipole-dipole interaction ($p_0\mathcal{E} \gg Np_0^2$). In the limit

$\tau_0 \gg T_2$, $\dot{W}/W$ calculated from (C5) is proportional to $\mathcal{E}^2$, which is a property consistent with predictions of nonlinear saturation, where $\mathcal{E}$ may be one of many possible pulse envelope functions. For very large τ_0, the effect of T_1 (spontaneous emission) must be taken into account, which is not included in (C4). The solutions (C5) satisfy Eq. (16) (for $d\langle\dot{\varphi}\rangle/dz = 0$) and the equilibrium relation (39). The solutions to the Bloch equations (8)–(10) are

$$
\begin{aligned}
u &= \frac{\eta c\sigma}{4\pi\omega}\left(\frac{\sqrt{2}}{\kappa\tau_0}\right)\operatorname{sech}\left(\frac{t'}{\tau_0}\right) , \\
v &= \frac{-\eta c\sigma}{4\pi\omega}\left(\frac{\sqrt{2}}{\kappa\tau_0}\right)\operatorname{sech}\left(\frac{t'}{\tau_0}\right) , \\
W &= \frac{\eta c\sigma}{2\pi\kappa^2}\,\frac{1}{T^2} - \frac{1}{\tau_0}\tanh\left(\frac{t'}{\tau_0}\right) , \\
W_0 &= \frac{\eta c\sigma}{2\pi\kappa^2}\left(\frac{1}{T^2} + \frac{1}{\tau_0}\right) .
\end{aligned}
\qquad \text{(C6)}
$$

Note that the number density N of dipoles contained in W_0 specifies a corresponding equilibrium pulse width τ_0.

Whereas the unchirped π h. s. solution is valid for $\sigma/\alpha_0 < 1$ and $1/\tau_0 = 1/\sigma'[1 - (\sigma'/T_2)]$ positive only [where $\sigma' = (\sigma/\alpha_0)T_2$ and $\alpha_0 = 4\pi\kappa^2 T_2 W_0/\eta c$], the chirped solution (C5) holds for $1/\tau_0 = (1/2\sigma') - 1/T_2$ positive only, with $\sigma/\alpha_0 < \frac{1}{2}$.

Armstrong and Courtens[11] obtained a h. s. chirped solution for pulse propagation at resonance in which the dispersion of the background refractive index η is taken into account. Their solution appears similar to ours above but the physical situation is quite different.

Since no physical system is restricted to two levels, a true nonlinear treatment, taking into account the background refractive index, should include all quantum transitions of the system.

---

*Research supported by the National Science Foundation.

†Submitted in partial fulfillment of the requirements for the degree of Doctor of Philosophy.

[1](a) J. C. Diels and E. L. Hahn, Bull. Am. Phys. Soc. **17**, 47 (1972); (b) Seventh International Quantum Electronics Conference, Montreal, 1972 (unpublished); (c) Third Rochester Conference on Coherence and Quantum Optics, 1972 (unpublished).

[2]S. L. McCall and E. L. Hahn, Phys. Rev. **183**, 457 (1969).

[3]With another definition for the average frequency ($\dot{\varphi}$ weighted by $\mathcal{E}$ instead of $\mathcal{E}^2$) a similar pulling tendency has been computer calculated by J. D. Diels [Phys. Lett. A **31**, 111 (1970)].

[4]F. A. Hopf, G. L. Lamb, Jr., C. K. Rhodes, and M. O. Scully, Phys. Rev. A **3**, 758 (1971); initial experimental results reported at the Montreal and Rochester Conferences, see Refs. 1(b) and 1(c).

[5]F. A. Hopf (private communication).

[6]J. C. Diels, Phys. Lett. A **36**, 26 (1970).

[7]F. T. Arecchi and R. Bonifacio, IEEE J. Quantum Electron. **QE-1**, 169 (1965); J. A. Armstrong and E. Courtens, IEEE J. Quantum Electron. **QE-4**, 411 (1968).

[8]L. Davidovich and J. H. Eberly, Bull. Am. Phys. Soc. **15**, 506 (1970); Opt. Commun. **3**, 32 (1971).

[9]R. E. Slusher and H. M. Gibbs, Phys. Rev. A **5**, 1634 (1972).

[10]T. M. Pierce and E. L. Hahn, Bull. Am. Phys. Soc. **17**, 47 (1972).

[11]J. A. Armstrong and E. Courtens, IEEE J. Quantum Electron. **QE-5**, 269 (1969).